Report No. FHWA-RD-76-173

QUICK RELEASE PULLBACK TESTING AND ANALYTICAL SEISMIC ANALYSIS OF A SIX SPAN COMPOSITE GIRDER BRIDGE

August 1976

Final Report

Document is available to the public through
the National Technical Information Service,
Springfield, Virginia 22161

Prepared for
FEDERAL HIGHWAY ADMINISTRATION
Offices of Research & Development
Washington, D. C. 20590

DISCLAIMER NOTICE

This document is disseminated under the sponsorship of the Department of Transportation in the interest of information exchange. The United States Government assumes no liability for its contents or use thereof.

The contents of this report reflect the view of the author, who is responsible for the facts and the accuracy of the data presented herein. The contents do not necessarily reflect the official views or policy of the Department of Transportation.

This report does not constitute a standard, specification, or regulation.

TECHNICAL REFERENCE CENTER
Turner-Fairbank Hwy Res Cntr
FHWA, Room A200
6300 Georgetown Pike
McLean, VA 22201

Technical Report Documentation Page

1. Report No.	2. Government Accession No.	3. Recipient's Catalog No.
FHWA-RD-76-173		

4. Title and Subtitle

Quick Release Pullback Testing and Analytical Seismic Analysis of a Six Span Composite Girder Bridge

5. Report Date: August , 1976

6. Performing Organization Code

8. Performing Organization Report No.

7. Author(s): Bruce M. Douglas

9. Performing Organization Name and Address

University of Nevada
Civil Engineering Department, Reno, Nevada 89557

10. Work Unit No. (TRAIS): FCP 35A2042

11. Contract or Grant No.: DOT-FH-11-8311

13. Type of Report and Period Covered: Final Report

12. Sponsoring Agency Name and Address

Federal Highway Administration
Office of Research
Washington, D. C. 20590

14. Sponsoring Agency Code: S0576

15. Supplementary Notes

FHWA Contract Manager, James D. Cooper (HRS-11)

16. Abstract

A six span four hundred and fifty foot long continuous composite girder bridge has been subjected to extensive dynamic testing to identify its structural dynamic properties. Transverse motions were induced by quick release pullback testing and vertical motions were induced by normal vehicular traffic. Analysis of the data obtained indicates that this type of dynamic testing is very effective for bridge structures of this type.

After obtaining the experimental dynamic properties, a linear analytical model was used for purposes of comparison with the experimental results and for estimating the seismic forces induced by small to moderate earthquakes having recurrence times on the order of 30 to 40 years in Western Nevada. Results of this analysis indicate that the earthquake forces prescribed by the AASHTO specifications (1961), under which this bridge was designed, are too low for seismic regions of the Western United States. The 300-pound per linear foot minimum transverse wind load controlled in the design, but dynamic seismic analysis indicates that lateral forces in excess of four or five times those caused by the wind loads would be expected to occur every 30 to 40 years. The peak ground motions associated with the earthquakes used in this study are about 14 percent of the largest ground motions ever recorded during an earthquake.

17. Key Words	18. Distribution Statement
Earthquake, experimental, dynamic, analysis, bridge seismic analysis.	No restrictions. This document is available through the National Technical Information Service, Springfield, Virginia 22161.

19. Security Classif. (of this report)	20. Security Classif. (of this page)	21. No. of Pages	22. Price
Unclassified	Unclassified	80	

Form DOT F 1700.7 (8-72)

Reproduction of completed page authorized

PREFACE

The investigation with interpretation as described in this report was sponsored by the U.S. Department of Transportation, Federal Highway Administration, under contract No. DOT-FH-11-8311 covering the period March 28, 1974 through March 31, 1976.

The general investigation called for in this contract is under the supervision and technical responsibility of Professor Bruce M. Douglas who acts as principal investigator.

LIST OF TABLES

TABLE OF CONTENTS (cont.)

TABLE OF CONTENTS

ACKNOWLEDGEMENT

The author wishes to express his most sincere appreciation to James D. Cooper, structural research engineer with the U.S. Department of Transportation, Federal Highway Administration for his patience, assistance and helpful comments during the course of this investigation.

In addition, the author wishes to thank Harlan Fricke, of S.E. and A. engineers for his efforts during the time he was a research assistant on the project.

Finally, thanks are also due the State of Nevada Department of Highways for their cooperation and help during the course of the investigation. In particular, Hugh Brinson and Al Westall were especially helpful.

LIST OF FIGURES

I. INTRODUCTION

Many highway bridge structures of various types were damaged during the 1971 San Fernando earthquake (17, 11). As a result of the damage that occurred, it became apparent that the seismic design criteria for bridges needed immediate review, and that new research studies of the dynamic performance of bridge structures during earthquakes were necessary. A worldwide literature search of the subject was initiated, and a complete bibliography of seismic effects on bridges was developed (16). Subsequently, Tseng and Penzien (27), and Chen and Penzien (7) have analytically examined the response of bridges representative of those structures damaged during the San Fernando earthquake. They have included linear and nonlinear behavior in their analytical models, as well as soil-structure interaction effects. Godden (12) is conducting sophisticated nonlinear model analyses of one of the long-span bridges which collapsed during the San Fernando event, and one for which a comphrehensive analytical model has been developed (27).

With regard to dynamic testing of the lateral dynamic behavior of existing bridges, the Japanese (16) have done most of the previous work. Shepherd and Sidwell (20) and Shepherd and Charleson (19) have performed resonance tests using steady-state sinusoidal excitation on several concrete bridges in New Zealand.

The experimental objectives of this study were to

determine the linear lateral dynamic properties of a continuous composite girder bridge by using quick-release pullback testing and the vertical dynamic properties by using the random traffic induced vertical motions. The main thrust of the work was to obtain the lateral properties, but because of the relative ease with which the additional vertical motion data could be obtained, the vertical motion study was appended.

The analytical objectives of the study were to compare the experimentally determined dynamic properties with those obtained from a linear analytical model. After the differences between the analytical model and the experimental data were resolved, the final objective was to use the linear analytical model to compute the earthquake dynamic response of the structure. The input earthquake accelerograms selected were chosen to represent the frequently occurring ground shaking for which the structure could be expected to respond in the linear range.

II. RAMP 13

A. DESCRIPTION

The structure chosen for this study was the Ramp 13 bridge structure in the interchange complex at the intersection of US 395 and I-80. The structure is illustrated in Fig. 1 and a plan and elevation are shown in Fig. 2. It carries one lane of traffic, and is the access ramp to US 395 south for eastbound traffic on I-80.

The structure is a six span continuous composite steel and concrete girder bridge supported on concrete piers and abutments. The overall length of the bridge is four hundred and fifty feet, and the total width is twenty-six feet. The reinforced concrete deck rests on three continuous steel plate girders spaced 9.68 feet apart. The ultimate strength specified for the deck concrete was 4000 psi. Because of the presence of a number of flange plates having different thicknesses at the top and bottom of each steel girder in each span, the composite deck is quite nonprismatic with respect to bending caused by vertical loads. In addition, the steel shear connectors which act at the interface of the steel girder and the concrete deck are spaced to achieve full composite action in the regions of positive moment. In the negative moment regions over the pier supports, the shear connectors are spaced at two foot intervals. This wide spacing is used at the ends of all interior

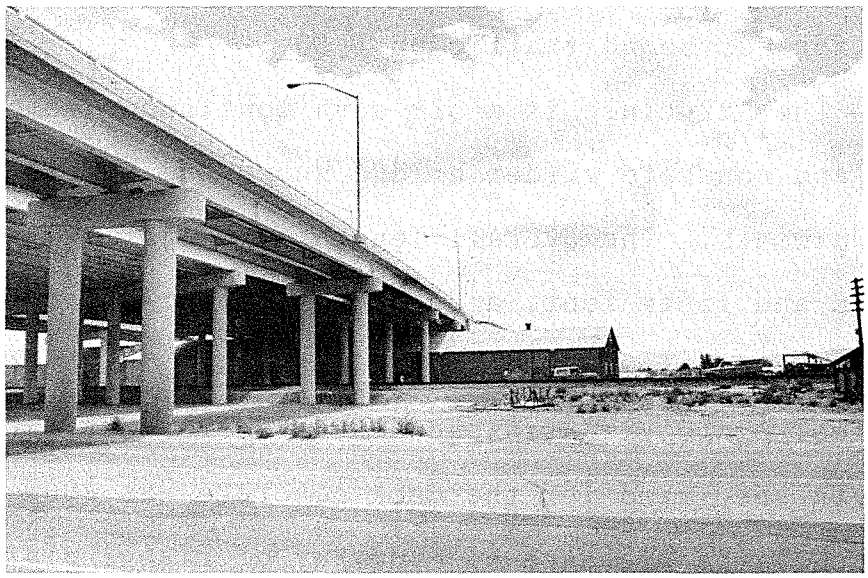

Fig. 1 Ramp 13

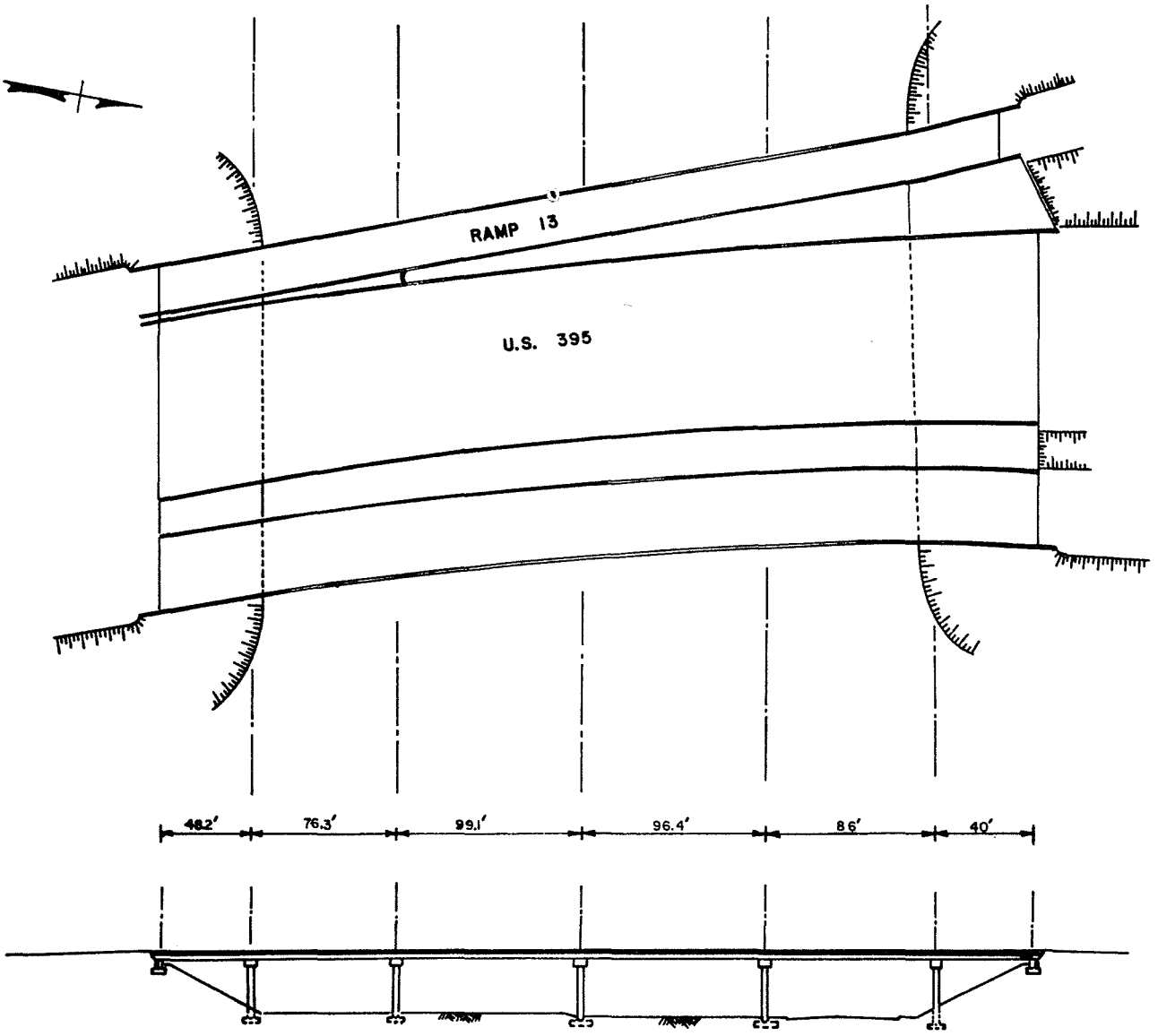

Fig. 2. Plan and Elevation

(Piers are numbered 1 to 5 consecutively from left to right)

spans for a distance approximately equal to fifteen percent of the span lengths.

Lateral loads are transferred from the deck to the piers and abutments by diaphram frames at each abutment and pier. These frames are formed by welding one inch thick bearing stiffeners to each side of the girder web plates. The frame is formed by bolting a 15 inch steel channel section between the interior bearing stiffeners. The bolted connections were of the friction type and have only a nominal moment resisting capacity. These diaphrams can be seen over the piers in Fig. 1.

The piers are reinforced concrete frames consisting of a horizontal pier cap rectangular in section supported by two circular columns. Each column is supported by an individual spread footing. The allowable bearing values for the spread footings was 6000 psf and the ultimate strength of the pier concrete was specified as 3000 psi. The center line dimensions for the pier frames are listed in Table 5.

The piers are numbered consecutively from south to north, and piers 1, 2 and 5 have three foot diameter columns while piers 3 and 4 have 3.5 foot diameter columns. The deck is rigidly connected to piers 3 and 4 by fixed bearings and at the remaining piers and abutments each girder is supported by a 12 inch high rocker which is 2.5 inches thick and 18 inches wide. This allows all of the thermal expansion and contraction to take place relative to piers 3 and 4. The

clearance between the end of deck and the abutment walls is on the order of four inches in the summer. This means that all of the longitudinal loads caused by earthquakes are carried in cantilever action by the columns at piers 3 and 4 only until such time as the end of the deck comes in contact with the abutment walls.

In contrast, the lateral earthquake loads acting on the structure are carried out through all five piers and the two end abutments.

One final feature must be mentioned because its presence had an effect upon the experimental results. In the plan view shown in Fig. 2, a connecting median strip between Ramp 13 and the US 395 overcrossing structure can be observed to extend about 135 feet from the south end of these structures. This median is structurally connected to the deck of the US 395 structure and it rests on the Ramp 13 deck spearated by a tar paper bond breaker.

For larger displacements this median would allow relative motions to occur between the structures, but for the smaller displacements associated with this testing program, the presence of the median strip affected the results.

B. EARTHQUAKE INSTRUMENTATION

Since 1972, Ramp 13 has been instrumented with strong motion accelerographs. The instrumentation program has been sponsored by the Federal Highway Administration. Four triggered film recording accelerographs are in interconnected

operation. One of the accelerographs is located on a slab on grade in the storage shed (Fig. 1) under the bridge between piers 1 and 2. The purpose of this instrument is to record the input ground motion to the structure. Another instrument is located at the north abutment and records the motion of the north abutment wall. The remaining two accelerographs record the structural response at piers 3 and 4 where the deck is rigidly fixed to the piers.

In addition to the four accelerographs four seismoscopes are in operation. A reference seismoscope is located with the accelerograph on grade in the storage shed. Another is located 300 feet north of the reference seismoscope at the foot of the north abutment. The remaining two seismoscopes are located 800 feet and 1300 feet away on roughly the north-south line through the reference seismoscope. It is hoped that the seismoscopes can be used to identify possible differences in ground motion with respect to the base station.

III. EXPERIMENTAL ANALYSIS

A. DATA ACQUISITION

1. General. A number of experimental dynamic analyses of building structures have been made using their ambient vibrations caused by wind or other random causes (3, 21, 24, 13, 22). The general procedures for data acquisition and analysis used in this study were taken from these references. Lateral ambient vibrations were not used in this case, because these vibration amplitudes were too small (less than .001 g acceleration) to be accomodated by the available equipment. It was for this reason that quick-release pull testing was considered as a means of exciting vibrations large enough to be recorded on the equipment at hand. In addition, when ambient vibrations are used, it is more difficult to produce reliable estimates of the structural damping ratios (24, 22, 14); but with quick-release pull testing it is a relatively simple matter to obtain modal damping estimates (15).

2. Excitation. To induce lateral vibrations having amplitudes large enough to be useful, the D-8 Caterpillar tractor shown in Fig. 3 was used to pull a 3/4 inch wire rope attached to the drawbar of the tractor and one of the piers of the bridge. The desired cable tensions were achieved to within 1000 pounds by simply using the lowest gear ratio and having the tractor crawl up to the desired load level.

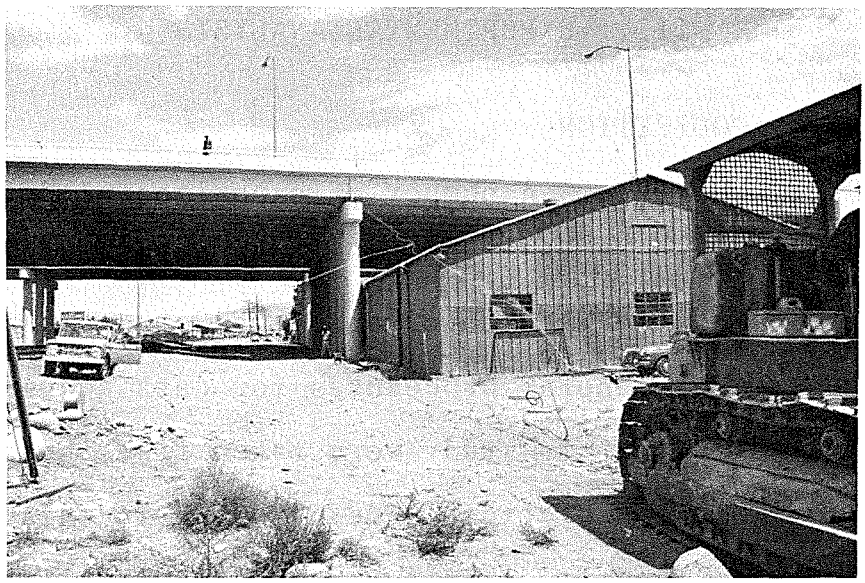

Fig. 3 D-8 Tractor Used For Pulling Loading Cable

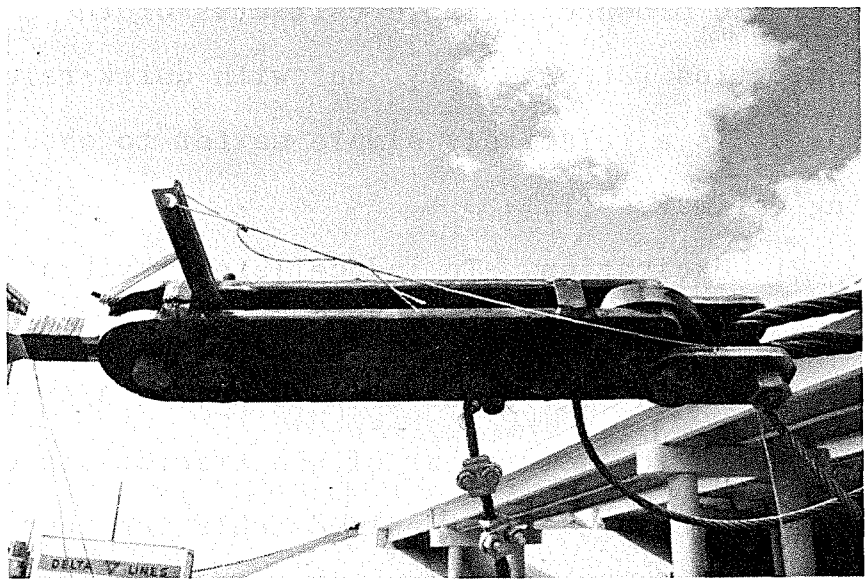

Fig. 4 Mechanical Quick-Release and Load Cell

A loading frame was fabricated from structural angle sections for purposes of securing the cable to the bridge piers. It was made to enclose the 12 by 24 inch steel masonry plate beneath the outside steel girder at the piers, and was designed for ease of movement from one pier to another. This frame was also designed with an extension so that the cable contact point was two inches away from the edge of the horizontal concrete pier cap. The two inch clearance was adequate to prevent damage to the wire rope and scarring of the concrete pier.

To achieve quick-release of the wire rope cable, a mechanical quick-release and load cell was designed and thoroughly tested in a universal testing machine up to loads of 22 kips. This device is shown in Fig. 4 and consists of a cable grip formed by slots cut into the outer frame and a mating slot cut in to the central wheel. When the mechanism is in use, the cable grip is slightly eccentric with respect to the tension axis. The slot on the wheel provides the release mechanism and it is triggered by a lever system having a mechanical advantage of 25 to 1 which releases a catch on the wheel. The load cell used was simply a short steel eye-bar with a pair of electric resistance strain gages mounted to minimize possible eccentricities occurring during use (left side of Fig. 4). To prevent the released cable from unsafe flinging after quick-release, restrainer cables were attached to the release mechanism and the free cable end.

The action of this restrainer cable may be seen in Fig. 3, which shows the loading cable the instant after it was released.

In the vertical motion portion of the study (10) only traffic induced motions were used.

3. Instrumentation and Experimental Procedures. Four Kistler force balance (305A-515) accelerometers were used to measure the bridge vibrations. The accelerometer signals were recorded at a central location on an Ampex (SP 700) four channel FM tape recorder without signal conditioning. Prior to electronic digitization of the acceleration data, it was filtered with a low pass filter having a 20 hz corner.

Acceleration data was taken at stations on the concrete barrier rail which was cast after the deck concrete had cured. The rail and deck act as an integral unit due to bond and the presence of reinforcement. The accelerometer stations were laid out at 10 foot intervals relative to the centerline of pier 3, and were numbered consecutively from south to north with the station at the centerline of pier 3 being station number 23.

The basic experimental procedure was to locate one of the accelerometers at a fixed reference station, and set up the remaining transducers at three consecutive stations. The cable was then loaded for quick-release. After the vibration data was obtained, the three moving accelerometers were set up at the next three stations leaving the reference

accelerometer in place. Quick-release vibration data was again obtained in the new setup. This process was continued until data had been obtained from all stations. Four separate sets of pull test data were used. Table 1 gives the location of the reference station, recording stations used, cable tensions, and pull point location for each test. During all of these experiments, the peak transverse accelerations induced by quick release pull testing ranged between 0.5 to 1.0 percent of gravity.

Table 1. Data Sets Used in This Study

Data Set	Reference Station	Pull Point	Cable Tension	Recording Stations
1	23	Pier 3	5^k	All at 10 ft. Spacing
2	23	Pier 2	5^k	Alternate at 20 ft. Spacing
3	23	Pier 3	12^k	Alternate at 20 ft. Spacing
4	23	Pier 2	12^k	Alternate at 20 ft. Spacing

B. MODE SHAPES AND FREQUENCIES

1. Data Analysis. In order to extract natural frequency and mode shape information from the experimental accelerogram data, the Fourier transform was used. An extensive analysis of the properties of the Fourier transform may be found in the book by Bracewell (4), and a shorter summary of its salient characteristics has been presented by Trifunac and Udwadia (5). A fast and efficient method of computing the Fourier transform was developed by Cooley and Tukey (8). Application of the Fourier transform in ambient vibration studies for purposes of extracting frequency and mode shape information from time series data obtained in ambient vibration studies has been detailed by Trifunac (24) and Benuska (3). For purposes of extracting mode shapes and frequencies, the pull test data was analyzed by techniques similar to those used in ambient vibration studies.

The four channels of FM recorded accelerogram data was prepared for analysis by first applying an electronic low pass filter with a 20 hz corner frequency. After removing the high frequency noise, all four channels of data were digitized simultaneously at a sample rate of 125 samples per second. Each digital record retained for analysis was 8.2 seconds long containing 1024 points. All of the pull test data indicated in Table 1 was processed in this manner and stored on magnetic tape compatible with the CDC-6400 digital computer.

For purposes of determining the natural frequencies and mode shapes the Fourier amplitude spectra (Modulus of Fourier transform) of each digital record was computed using the Cooley-Tukey (8) algorithm. Finally, Hanning smoothing using the weights (1/4, 1/2, 1/4) was applied to each spectral ordinate. Hanning smoothing with these weights is equivalent to using a cosine bell window in the time domain (5). A phase spectrum was also calculated for each digital record. Then, for each quick release setup indicated in Table 1, an amplitude ratio spectrum was tabulated by dividing the spectral ordinates obtained at the variable recording stations by the spectrum obtained at the reference station, and a phase difference spectrum was formed by subtracting the phase spectrum of the reference station from the phase spectrum obtained at each variable recording station.

Natural frequencies were estimated from the direct Fourier amplitude spectra, and mode shapes were extracted by using the phase difference spectra for identifying the arithmetic sign of the mode and the modal amplitudes were obtained from the ratio spectra at the modal frequency.

2. Transverse Natural Frequencies. To identify the transverse natural frequencies of Ramp 13, amplitude spectra obtained at reference station 23 were used. From data set 1, when the pull and release point was located at pier 3, twelve amplitude spectra were averaged, and this result is shown as the solid line in Fig. 5. In addition, six spectra from data

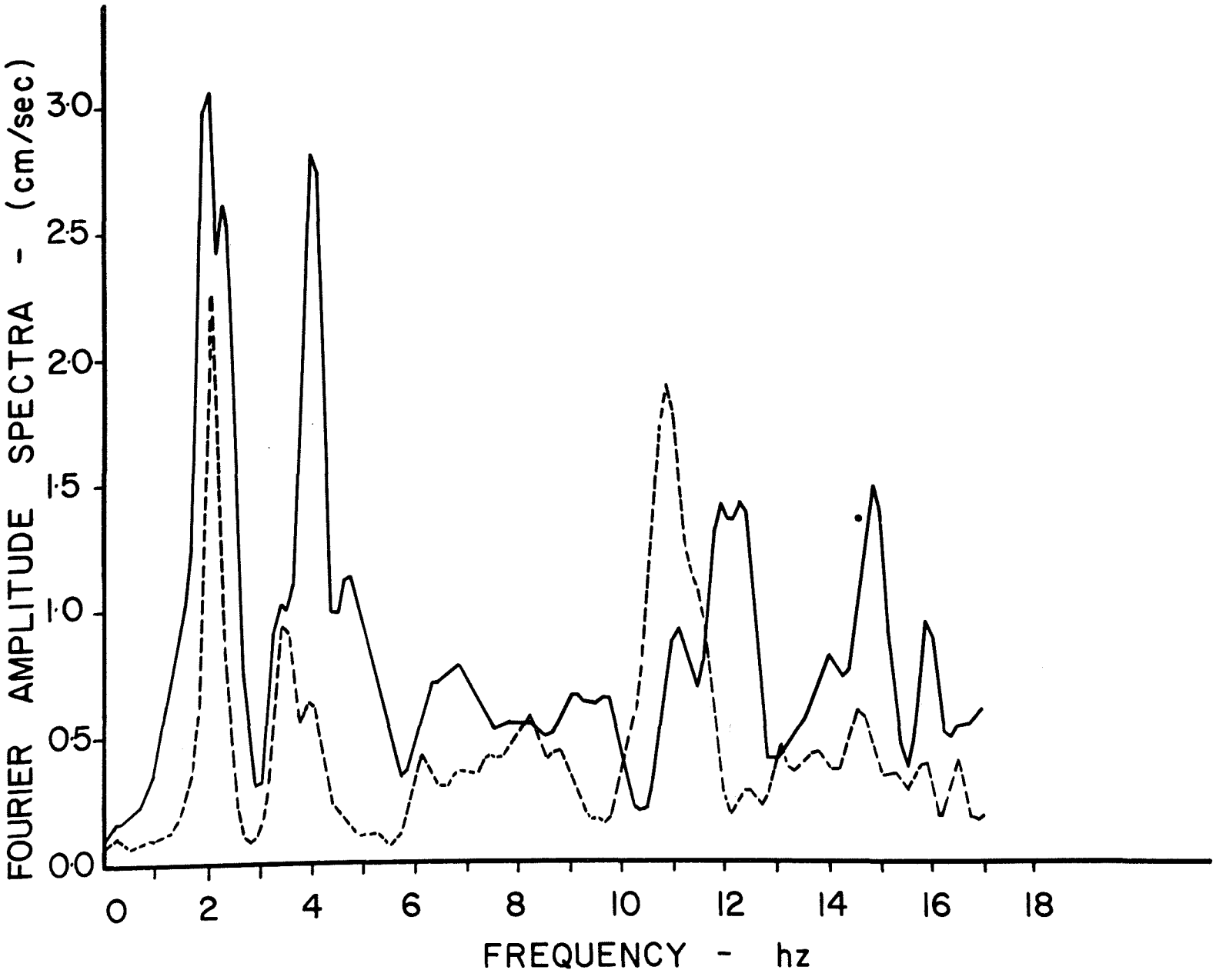

Fig. 5 Average Fourier Amplitude Spectra: Solid Line - Data Set 1, Dashed Line - Data Set 2.

set 2, with the pull and release point at pier 2, were averaged resulting in the dashed curve shown in Fig. 5. More samples were available in data set 1 because the station spacing used in that experiment was one half that used in data set 2.

From Fig. 5 it is apparent that the frequency content of the spectra varies depending upon the location of the pull point, since the only difference between the two data sets was pull point location. The amplitudes of the spectral peaks would be expected to depend upon the initial configuration of the structure which is controlled by the location of the pull and release point, but the modal frequencies should not be different because the initial configuration from which the structure is released varies.

From the dashed curve in Fig. 5 it is clear that the fundamental mode is clearly excited at 2.08 hz. In this case, the pull point was at Pier 2. From the solid spectrum in Fig. 5 with the pull point at Pier 3, it is clear that there are two neighboring frequencies at 2.08 hz and 2.32 hz. In the next section it will be shown that these frequencies are related to two distinct transverse fundamental mode shapes; and in the chapter on theoretical mode shapes it will be shown that the presence of the 135 foot median strip on the southern end of the bridge is the explanation of this nonunique dynamic behavior. It is also clear from Fig. 5 that the higher modes also exhibit this multiple frequency

nonunique behavior, and that it is more pronounced when the pull point is at pier 3 as compared to pier 2.

The lowest frequency found for each of the first five modes is tabulated in Table 2, and from Fig. 5 it can be seen that peaks exist at these frequencies in the first, second and fifth modes on both spectra. In the case of the third and fourth modes, these frequencies are only clearly identifiable in the dashed curve.

Table 2. Natural Frequencies

Mode	1	2	3	4	5
Frequency (hz)	2.08	3.42	6.10	8.18	10.86

3. Transverse Mode Shapes. A total of six distinct transverse mode shapes were determined from the data and are shown in Figs. 6-8. Additional shapes at higher frequencies could have been presented, but they were not included because only the lower modes are structurally significant when attempting to describe the earthquake response of linear structural systems.

Two forms of the fundamental mode are shown in Fig. 6, where the upper curve represents the 2.08 hz mode and the lower curve is the mode at 2.32 hz. These two neighboring fundamental frequencies can clearly be seen in the

spectra (Fig. 5). The solid black dots in the upper curve were obtained from the ordinates of the ratio spectra calculated from data set 2, and the solid black arrow indicates the pull point location for that suite of data. It is obvious from the dashed spectra in Fig. 5 that this data should produce a very well defined mode. The hollow circles were obtained from the ratio spectra of data set 1 which had a station spacing of 10 ft. with the pull point at pier 3. This data also defined this mode very well. The lower curve in Fig. 6 defines the mode shape at 2.32 hz, and both sets of data points shown were taken from data set 1 with the pull point at pier 3. The hollow circles were obtained from the spectral ratios at 2.32 hz, while the solid circles were obtained from the 2.44 hz spectral ratios. Where both data points are not visible, the points are coincident. Trifunac (24) points out that spectral ratios at adjacent frequencies may be used to resolve mode shapes having nearly the same frequencies. Also, it is a relatively simple theoretical matter to show that mode shapes may be recovered by using spectral ratios anywhere within the spectral peak defining the mode when pull test data is used. To illustrate this, the lower mode shape was established by using the spectral ratios at 2.44 hz from the data associated with the dashed spectra in Fig. 5. From that figure it can clearly be seen that there is no peak at all at 2.44 hz. These spectral ratios clearly defined the mode to the right of

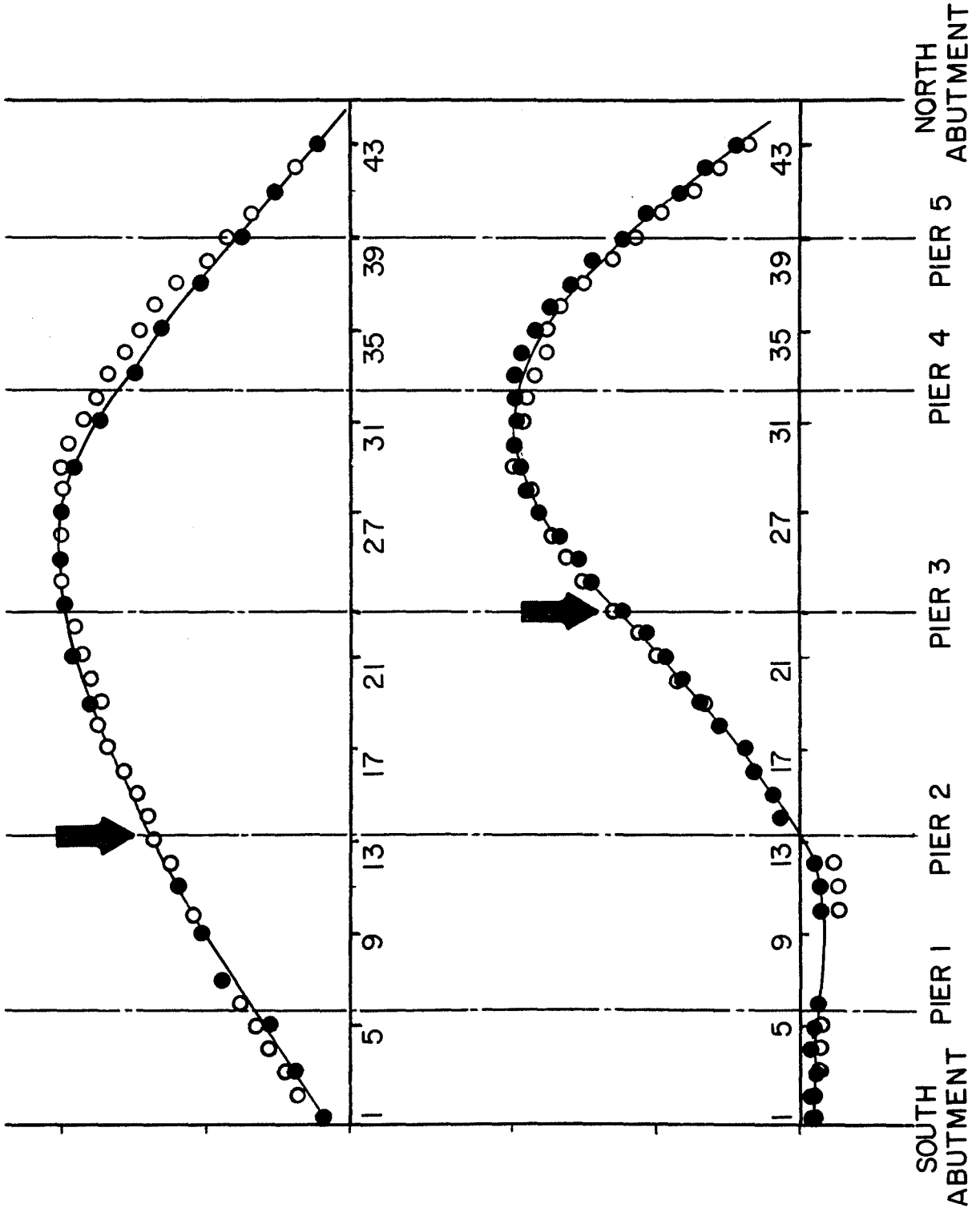

Fig. 6 Fundamental Mode Shapes - The Upper Curve Is The 2.08 hz Mode and the Lower Curve is the 2.32 hz Mode.

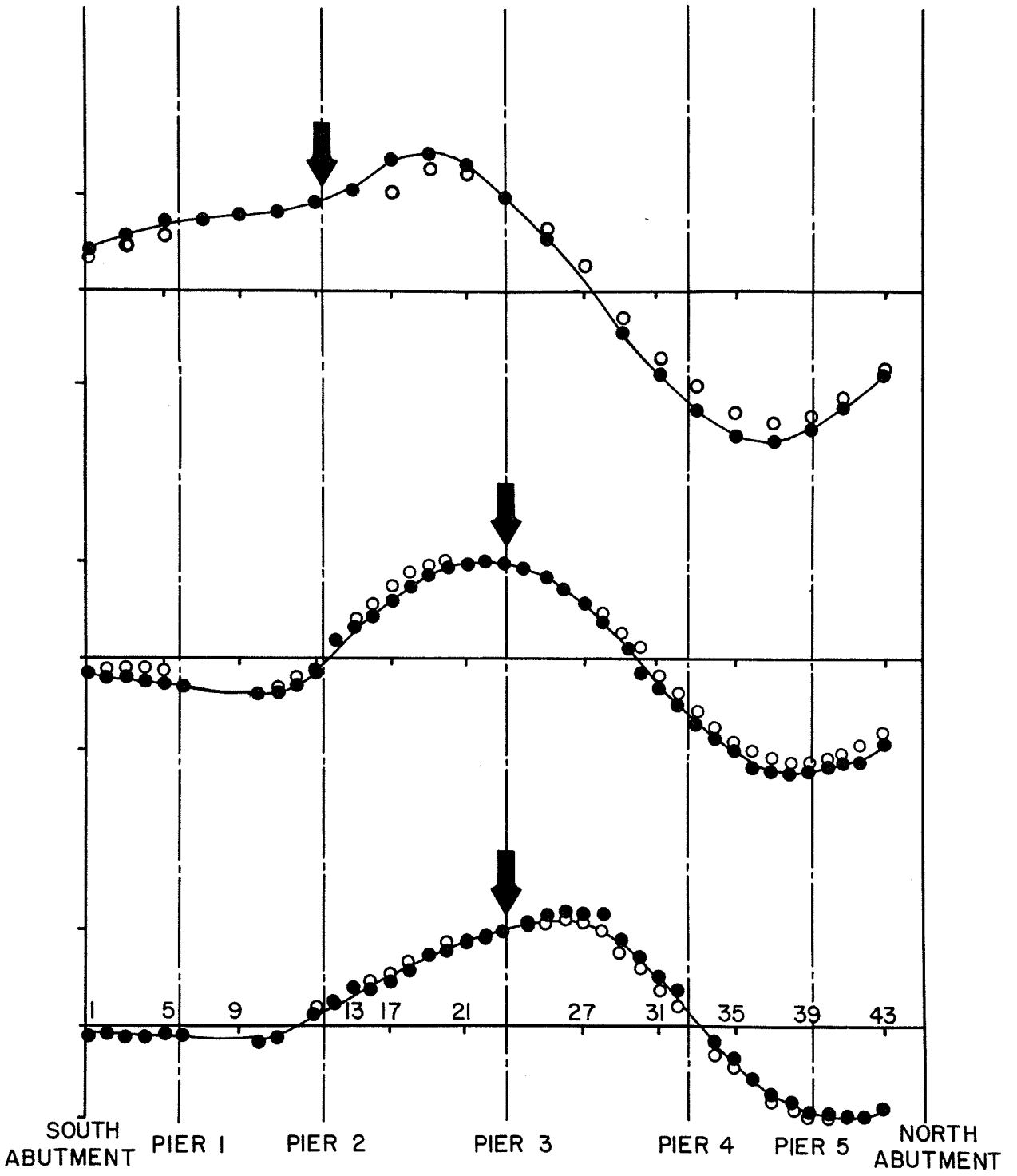

Fig. 7 Second Modes - Upper Curve - 3.42 hz Mode, Middle Curve - 4.03 hz Mode, and the Lower Curve - 4.76 hz Mode.

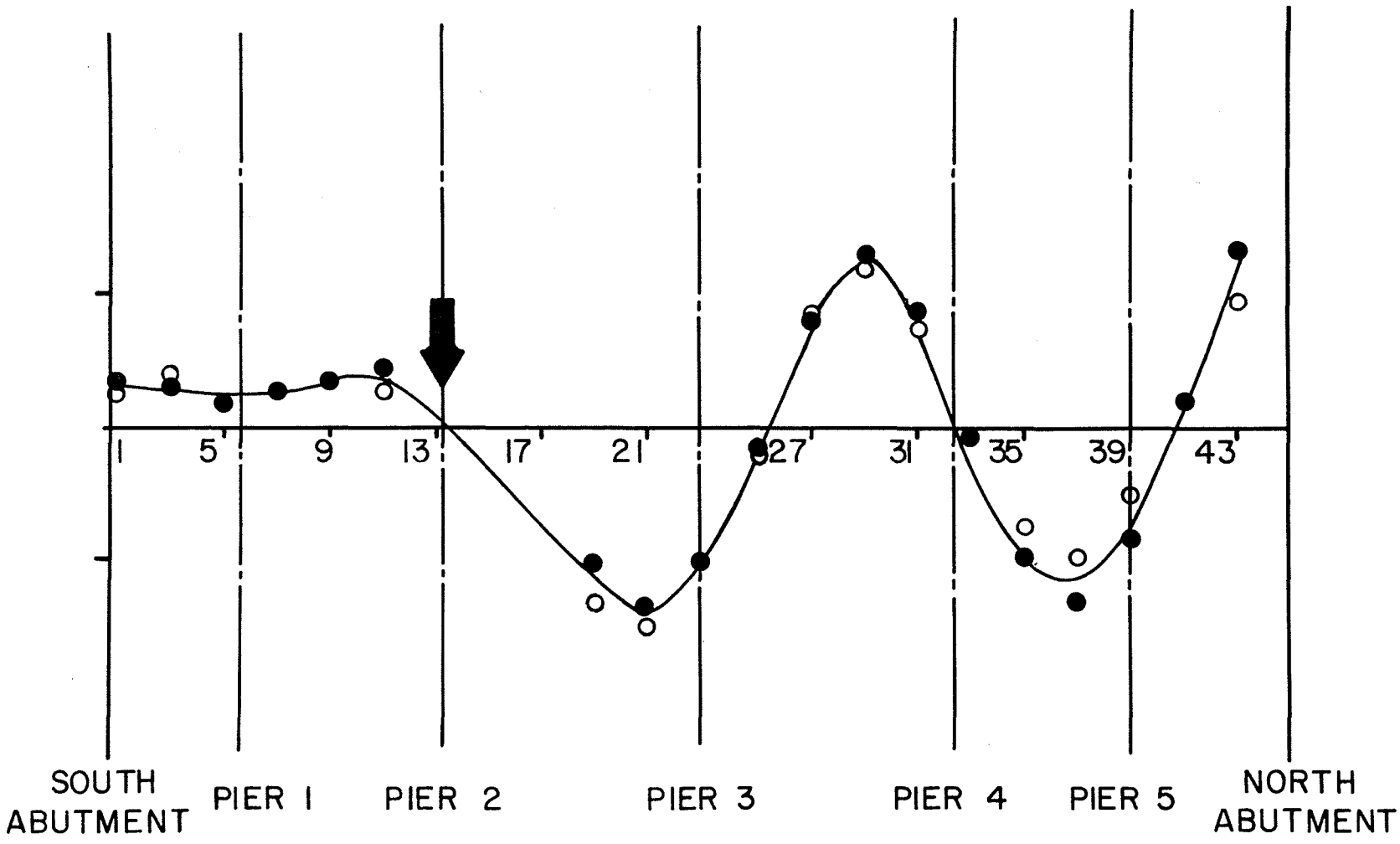

Fig. 8 Fifth Mode at 10.86 hz.

pier 2; but gave erroneous results due to limited vibration amplitudes in the region containing the median strip between the south abutment and pier 3.

The nonunique dynamic behavior exhibited by this structure, which is indicated by the existence of multiple forms of each mode of vibration at frequencies close to each other, is caused by the presence of the median strip. The median terminates approximately at station 13, and Fig. 5 shows that when the pull point is at pier 2 the fundamental mode which involves the largest relative displacement of the median strip with respect to the deck of Ramp 13 is strongly excited, almost to the exclusion of the alternate form. When the pull point is at pier 3, both forms of the fundamental mode are strongly excited. In the higher frequency form, it is readily apparent that the median strip is restraining the transverse displacements over the southern 135 feet of the deck. In the chapter treating theoretical modes shapes, it will be shown that the restraining action of the median strip can account for this structures nonunique dynamic behavior at the amplitudes of vibration used in this study.

From the top down, Fig. 7 shows the three forms of the second mode that were isolated at 3.42, 4.03, and 4.76 hz respectively. The data points in the upper curve are taken from spectral ratios at 3.42 and 3.54 hz calculated from data set 2. Data points for the lower two curves in Fig. 7 were taken from spectral ratios calculated from data set 1.

Frequencies 3.91 and 4.03 hz were used for the middle curve, and 4.64 and 4.76 hz for the lower curve. Fig. 8 contains the fifth mode at 10.86 hz defined by data set 2.

The third and fourth modes were not clearly excited for either of the pull points; this is clear from an examination of Fig. 5. In addition to the frequency smearing obviously present in those two modes, the signs of the modal displacements were not uniformly consistent as indicated by the phase difference spectra. In this case, the action of the median strip essentially obliterated these modes.

C. MODAL DAMPING

1. Data Analysis. Quick release test data has been used by Hidalgo and Clough (15) to determine modal damping ratios of a two story reinforced concrete frame. In that study, the time series data was electronically bandpass filtered to isolate the two modal components of motion in the time domain. For each of these components, the logarithmic decrement was determined and the modal damping ratios estimated in the usual manner (23). In this study, due to the presence of the complex motions caused by the action of the median strip, it was decided that this approach for estimating the damping ratios would not be attempted. Instead, a moving window Fourier transform (26) was applied to the problem.

2. Moving Window Spectral Decay Curves. The Fourier transform used in this study has the form

$$F(\omega) = \int_{T_o}^{(T_o+L)} \ddot{y}(t)\ e^{-i\omega t} dt \qquad (1)$$

where $\ddot{y}(t)$ is the time series accelerogram for which the transform is being computed, L is the width of the window used in the spectral calculations and T_o is the initial time of the window L. T_o can also be thought of as the time after the onset of motion at which the spectral calculations are begun, ω is circular frequency and i is $\sqrt{-1}$.

The moving window Fourier analysis used to calculate damping ratios from the data was obtained by repeatedly calculating the Hanning smoothed Fourier amplitude spectra associated with the transform defined by equation (17). The Fast Fourier Transform (FFT) was used for this purpose (8). The window location in the time series, T_o, was incremented in small uniform increments while the window length L was held constant. In the standard 1024 point accelerogram, the total time duration of the sample is 8.184 seconds, and the moving window analysis on this standard sample was performed by using a window length L equal to half the total sample duration. Thirty-three successive Fourier spectra were calculated for each time series, moving the window down the time series in 32 uniform time increments of 0.128 seconds. This detailed analysis of the time series, allows one to investigate the frequency shift of the modal peaks as well as the

modal damping ratios.

From this set of 33 Fourier amplitude spectra, computed for one accelerogram, the decay of the modal spectral peaks as a function of time is determined by plotting the normalized peak amplitude of the mode against time measured in units of time equal to the undamped period of the mode in question. Damping estimates from these diagrams were made by comparing them to theoretical decay diagrams.

Figure 9 illustrates a plot of the theoretical amplitude decay versus initial window time for various damping levels. The theoretical moving window spectra used to develop these curves were obtained by using a single modal term associated with a damped simple oscillator and integrating as indicated in equation 1. When only a single modal term is used, the modal frequencies must be adequately separated to give valid results. For purposes of comparison with the data spectra, L was taken to be 4.088 sec., and account was taken of the fact that the theoretical spectra are functions of the window length L. To determine how sensitive the decay curves were to the window length L, curves of the type shown in Fig. 9 were generated for simple oscillators having frequencies between 0.5 hz and 30 hz. This range was chosen because it more than covers the range of significant natural frequencies associated with the Ramp 13 structure, which has a fundamental frequency of 2.08 hz. It was found that for frequencies higher than 2 hz, the theoretical amplitude

decay curves are negligibly dependent upon the 4.088 sec. window length, and these curves are shown in Fig. 9. At frequencies near 0.5 hz the decay curves depend more strongly on the window length L. This would be expected, since fewer cycles of these low frequency motions are contained in the fixed window length of 4.088 seconds. Also, the calculation becomes more sensitive to the position of the window in the time series. It is also of interest to note that the peak spectral amplitude decay curves shown in Fig. 9 are very closely approximated by the exponential envelope of the time series of the modal motion.

The moving window spectral decay curve method of obtaining modal damping estimates is illustrated in Fig. 10. At the top of the figure a typical quick release accelerogram is shown. In this case, the release point was at pier 2 and the accelerogram recorded at station 23. The 8.2 sec. window below the accelerogram indicates that portion of the record which was digitized for Fourier analysis, while the 4.1 sec. window to the right indicates the final window position. Spectral decay curves in the 2.08 hz fundamental mode and the 10.86 hz fifth mode computed from this accelerogram are also shown in Fig. 10. In each of these modes, the appropriate theoretical spectral decay curves are included for comparison with the data.

In the case of the fundamental mode, it is obvious that the damping ratio is between 1.5 percent and 2 percent

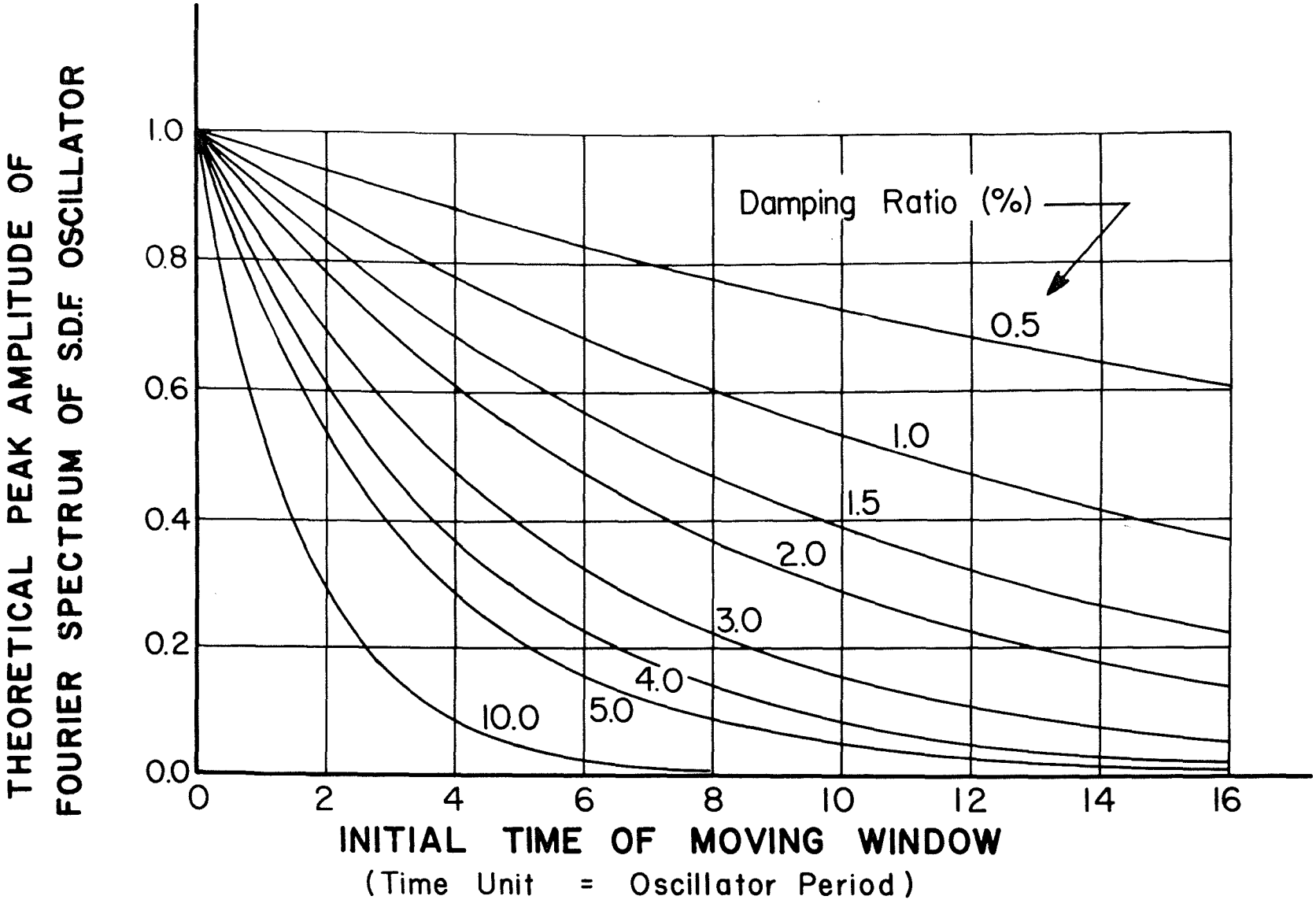

Fig. 9 Theoretical Moving Window Spectral Decay Curves.

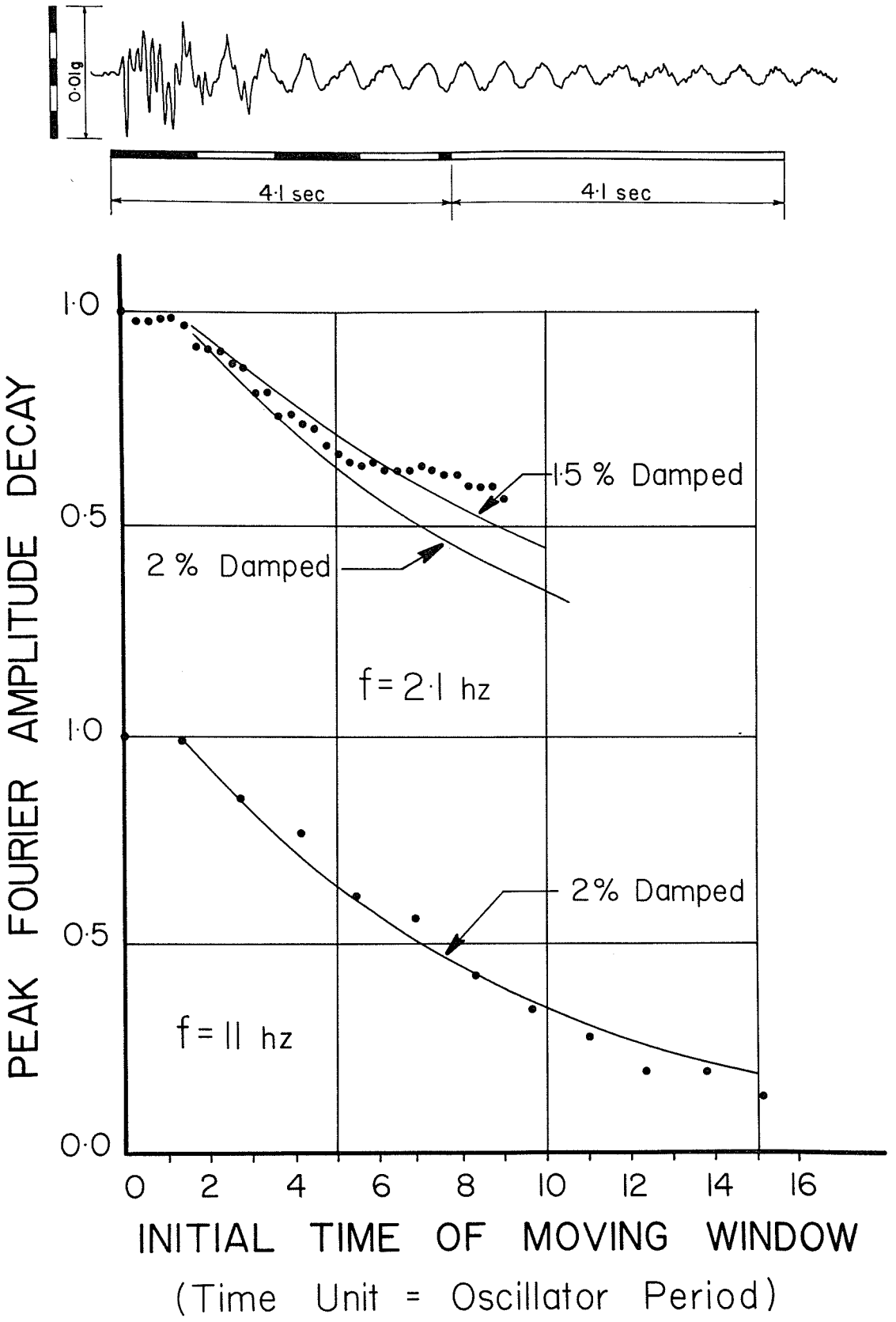

Fig. 10 Typical Quick Release Accelerogram and Associated Spectral Decay Curves.

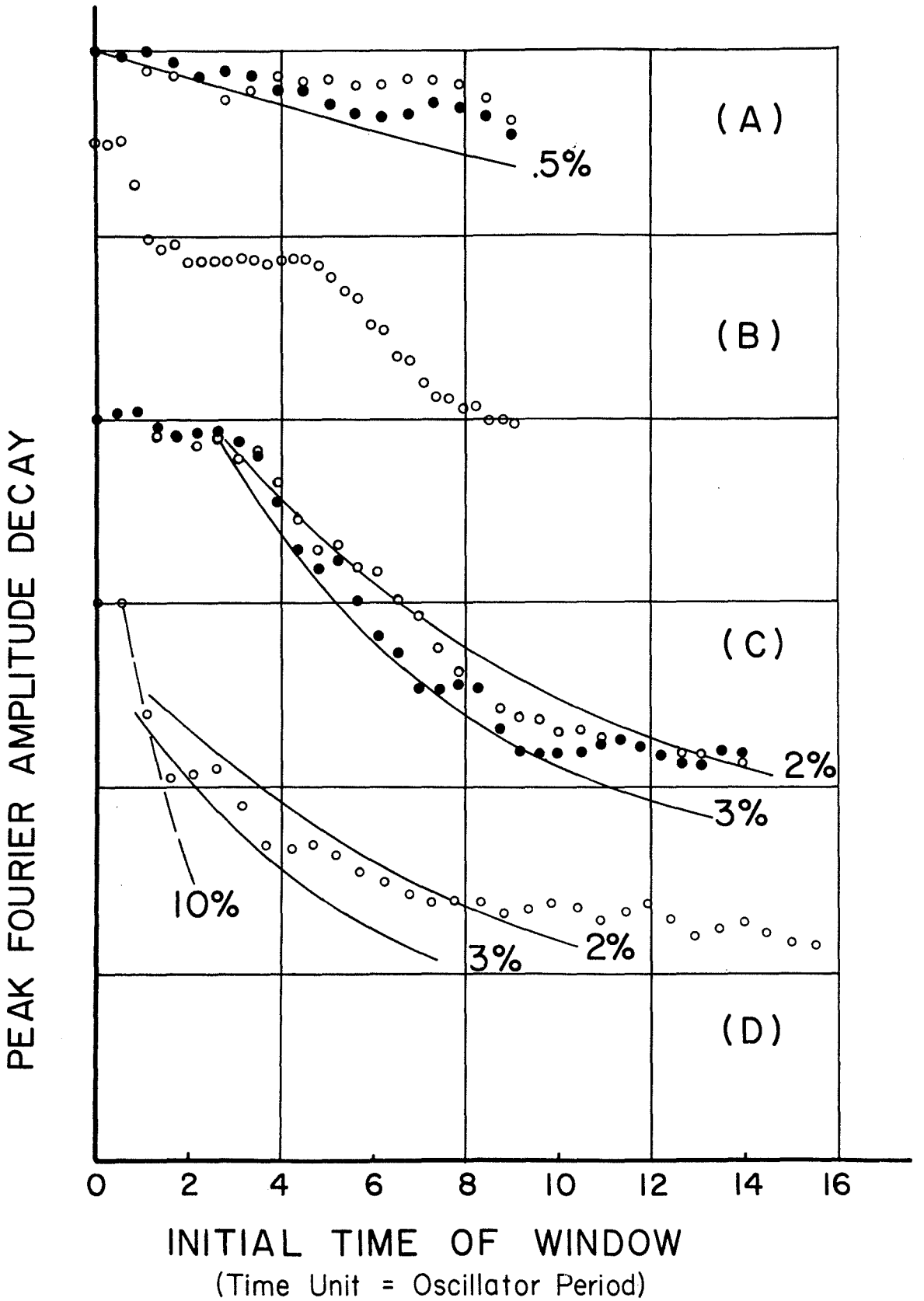

Fig. 11 Representative Spectral Decay Curves.

for the first six cycles of oscillation, and for the remainder of the record it is between 0.5 percent and 1 percent. Examination of the accelerogram indicates that after six or seven cycles, the fundamental mode is the only mode having large amplitudes in the accelerogram. Direct calculation of the fundamental modal damping ratio in this portion of the record by the logarithmic decrement method (23) gives a modal damping value of about 0.7 percent, which is in agreement with the value obtained for this portion of the record by the Fourier method. The lower curve in Fig. 10 shows these decay plots for the 10.86 hz fifth mode in which the damping ratio is two percent. The high frequency oscillations at the beginning of the accelerogram are associated with this mode, and the peak acceleration of 0.5 percent g is associated with this mode which is strongly excited by the quick release of the loading cable.

3. Experimental Results. Representative samples of the decay curves obtained in this study are illustrated in Fig. 11. Curve A represents the lowest damping ratio found in any mode for all tests, and it was anamolous in that all other damping estimates in all modes were 1 1/2 percent or greater. The hollow circles were calculated from the accelerogram obtained at station 23, while the solid dots are those determined from the record taken at station 33 during the same excitation.

Curve C also shows the damping curves for the 3.42

hz second mode calculated for station 5 (hollow circles) and station 23 (solid circles) during the same quick release excitation. A total of seven comparisons of this type were made, and the agreement between the spectral decay curves for different locations within a given excitation is typical of that shown in curves A and C. Linear vibration theory which assumes viscous modal damping, demands that the modal damping estimates made anywhere on the structure during the same excitation be identical. These results show that this assumption is valid for this structure, but that the modal damping may not necessarily be constant with time.

Curve D in Fig. 11 is a damping curve associated with the 4.03 hz form of the second mode. Curve B is a decay curve for the fundamental mode when both forms of the fundamental mode at 2.08 and 2.32 hz were strongly excited. The explanation for the anomolous shape of B is that the moving window spectral peak shifted from the lower frequency form to the higher frequency form with time as could be readily determined by the moving window analysis. In curve B, the steep left portion is associated with the lower frequency fundamental mode and the right hand part with the higher frequency form. The flat zone between them represents the time when the transition took place. Only those decay curves which were associated with the amplitude decay of the same mode (determined from the moving window analysis) were used for estimating the damping ratio. Decay curves of this type are illustrated in Fig. 10

Mode	Frequency 1 hz	No. of Separate Estimates	No. of Separate Excitations	Damping Range %	Damping Avg. %
1	2.08	9	5	0.5-3.0	1.7
1	2.32	5	4	1.5-4.0	2.8
2	3.42	3	2	2.0-3.0	-
2	4.15	1	1	2.5	-
5	10.86	2	2	1.5-2.0	-
5	11.96	3	3	2.5-4.0	-

Table 3 - Modal Damping Ratios

and A, C and D of Fig. 11.

A final comment regarding the flat portion at the left of some of the experimental decay curves is in order. This occurs because the windows over which the digital accelerogram was obtained do not always begin exactly at the onset of the motion, and it is a rough index of when the mode becomes strongly excited within the accelerogram.

Based on this method of analysis modal damping estimates were made for the 2.08 hz fundamental 3.42 hz and 4.15 hz second modes, and 10.86 hz and 11.96 hz fifth modes. Valid damping estimates were not possible in the third and fourth modes. The damping results are given in Table 3. Based on the results in this table, it can be seen that the damping ratios in all modes studied ranged between 0.5 percent and 4 percent. If the single anomolous estimate of 0.5 percent is excluded, the damping estimates range between 1.5 percent and 4 percent.

4. Damping Estimated From Widths of Spectral Peaks. In addition to the foregoing method of estimating damping, a method based on the width of the modal spectral peaks was attempted. When resonance testing is employed, a simple method of estimating damping from the width of the resonance curve at the half power point (23) is used. An analogous method was attempted in this study by deriving the width of the spectral peak at the half power point for quick release motions from theoretical considerations. Experimentally

determined widths were obtained from data spectra and compared to the theory. In the 18 cases examined, this experimental method gave damping estimates that were about a factor of 2 too high. The explanation for this is the fact that slight changes in the theoretical widths at the spectral peaks are associated with fairly large changes in the damping estimates for small damping values; and the fact that the frequencies probably drift slightly in quick release excitation. This would not be the case in resonance testing. This method was abandoned because it did not work well.

IV. THEORETICAL ANALYSIS

A. ANALYTICAL MODEL

After determining the system's dynamic properties experimentally, a linear lumped mass dynamic model was developed to predict these properties theoretically. The SAP IV (2) structural analysis program developed by the University of California at Berkeley was used for this purpose.

The composite reinforced concrete and steel girder deck is supported at the abutments and at piers 1, 2 and 5 by 12 inch high rocker bearings. At piers 3 and 4, the deck is attached by fixed bearings that prevent longitudinal movement relative to the pier caps. This allows the longitudinal thermal displacements to take place relative to piers 3 and 4. The clearance between the end of the deck and the abutment is three to four inches, depending upon the temperature. All longitudinal loads are resisted by piers 3 and 4 acting as vertical cantilevers relative to the 12 foot by 12 foot spread footings at the base of each of the 3 1/2 foot diameter pier columns. For these reasons a single degree of freedom dynamic model was used for the longitudinal motion, and it had a fundamental period of 1.3 seconds.

In the transverse sense, the system was treated as a lumped mass continuous beam restrained by transverse elastic supports which modeled the pier and diaphram frame elasticity. A four foot nodal increment was used. The deck was modeled

both as a continuous beam using the gross section of the deck concrete, and as a completely composite concrete and steel member using all the girder steel. Differences in the transverse mode shapes and modal frequencies for these two cases were negligible out through the fifth mode, and in all subsequent analyses the deck was treated analytically by using the gross section of the concrete only. As a final refinement, the effect of the 130 foot median strip alluded to previously, was modeled as a continuous lateral elastic support. The lateral stiffness per unit length of this elastic support was taken to be a constant with its total stiffness being measured in multiples of the total transverse stiffness of piers 1 and 2.

The reinforced concrete pier frames were analyzed by using their gross section stiffness properties and centerline dimensions. Since the pier frames had a relatively high height to width ratio (See Table 5) whose lateral stiffness could be affected by the soil stiffness both by overall rocking and rotation of the spread footings, this soil structure interaction problem was treated in an approximate manner by estimating the modulus of subgrade reaction using the procedures outlined by Richart and others (18) and Barkan (1). For this structure it was found that the lateral stiffness of the piers was sensitive to variations in the subgrade coefficient, and should therefore be included in the model. In the absence of soil test data, an average subgrade

coefficient of 450 kips per cubic foot was used for the full sized footings to provide for a nominal amount of foundation interaction. The fundamental period of the structure was increased 13 percent by including this nominal level of interaction; this phenomenon would be even more pronounced for softer soils.

The steel diaphram cross frames at each pier and abutment which transmit the lateral deck loads to the piers and abutments were treated as frames with moment resisting connections. The geometry of the members was such that the effect of shear deformation was quite significant, and for this reason was included in the analytical treatment. The total stiffness of lateral load carrying elements was obtained by including the action of both the piers and the diaphram cross frames.

B. ANALYTICAL MODE SHAPES AND NATURAL FREQUENCIES.

It was noted under the experimental section that the structure did not behave as a unique dynamic system, but had multiple transverse mode shapes and associated natural frequencies. At the top of Fig. 12 the two observed fundamental mode shapes at 2.08 hz and 2.32 hz are shown as the heavy curves (b) and (e) respectively. Also shown are the theoretical fundamental mode shapes (a), (c) and (d) which were calculated for a median strip stiffness of 0, 5 and 100 respectively (herein, median stiffness is measured in multiples of

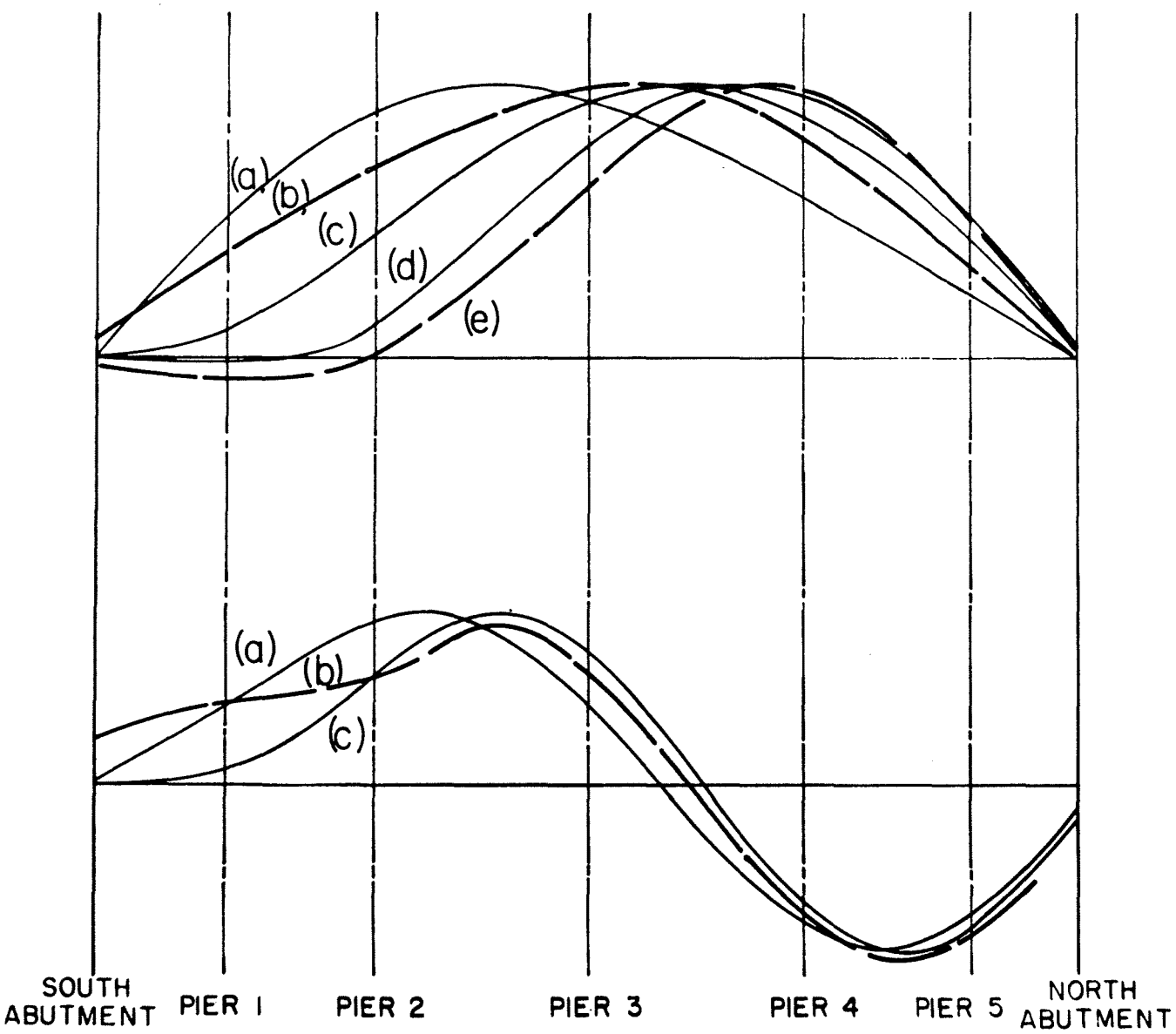

Fig. 12 Theoretical Modes Compared to Experimental Modes.

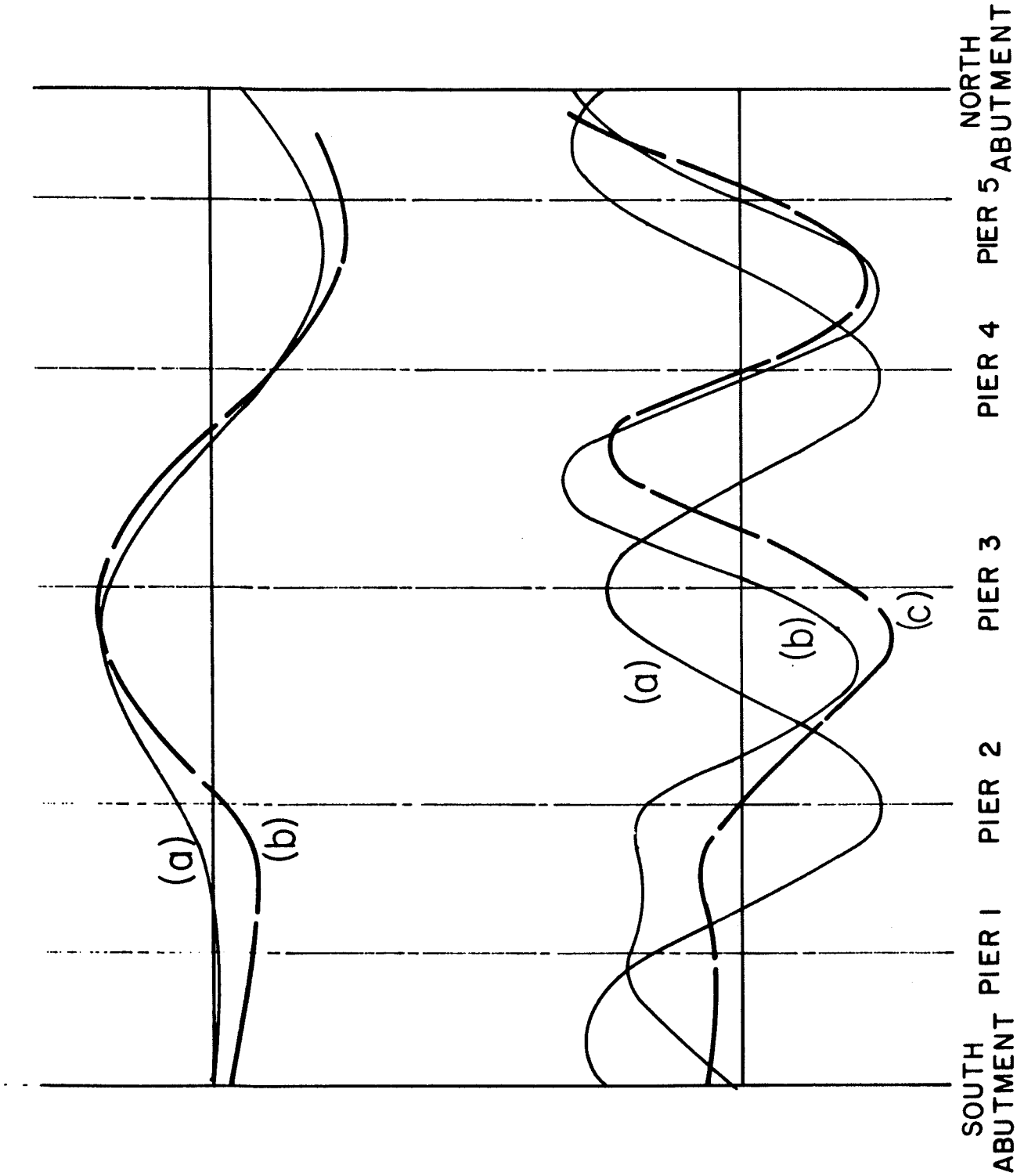

Fig. 13 Theoretical Modes Compared to Experimental Modes.

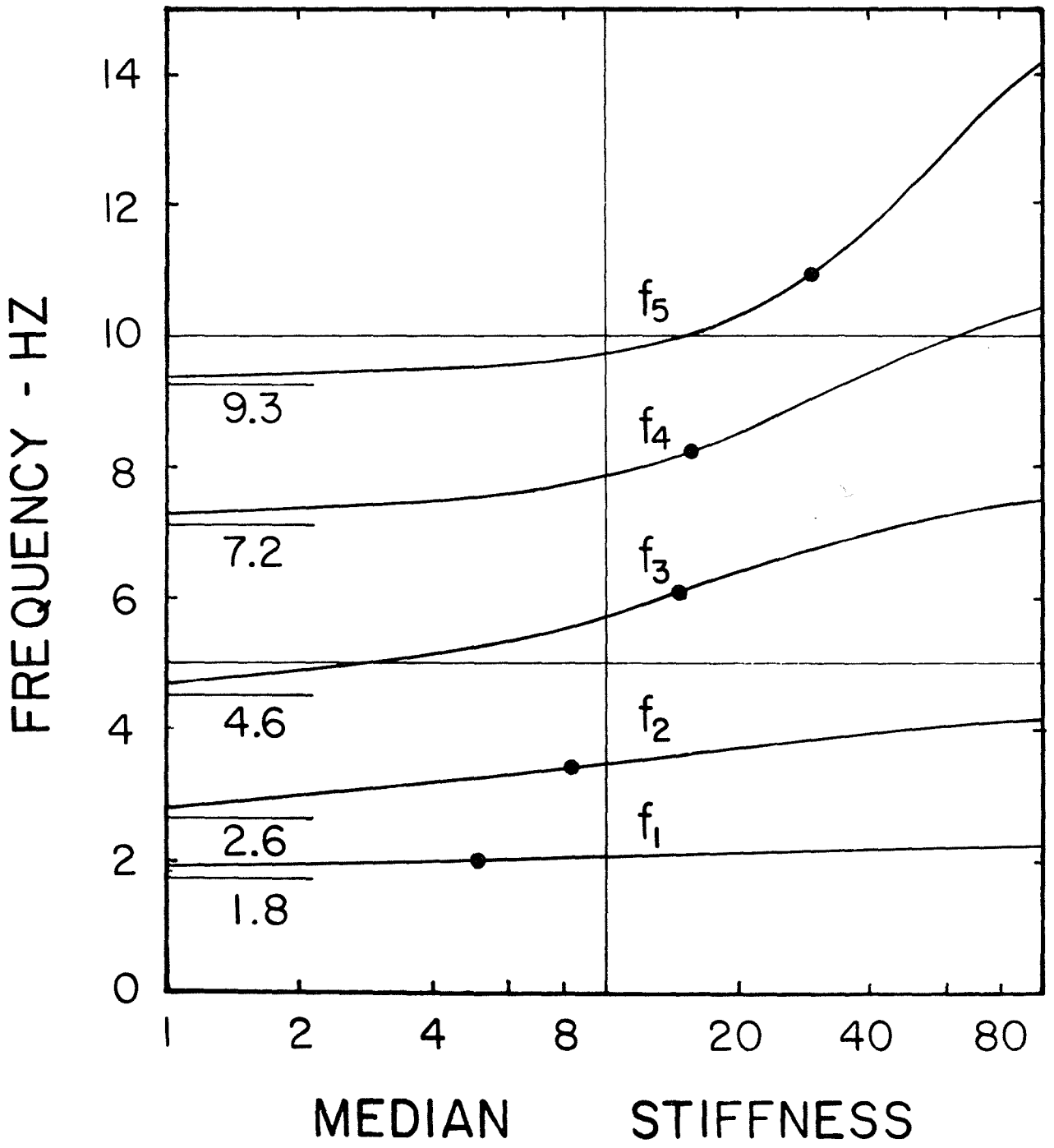

Fig. 14 Natural Frequencies as a Function of Median Restraint

the total transverse stiffness of piers 1 and 2). In the lower half of Fig. 12 the heavy curve (b) represents the experimental 3.42 hz second mode shown at the top of Fig. 7 compared to the theoretically determined mode shapes (a) and (c). Curve (a) represents the second mode when the median stiffness is 5 and (c) is the second mode when the median stiffness is taken as 20. The 4.03 hz second mode shown as the middle curve in Fig. 7 is drawn as the heavy curve (b) at the top of Fig. 13. Mode shape (a) at the top of Fig. 13 is the form of the theoretical second mode shape when the median stiffness is taken as 100. Modes (a) and (b) at the bottom of Fig. 13 represent the theoretical fifth mode when the median stiffness is zero and 100 respectively. The accompanying fifth mode shape (c) represents the experimental fifth mode at 10.86 hz shown in Fig. 8.

The first five transverse natural frequencies (f_1 to f_5) plotted as a function of the transverse median strip stiffness are shown in Fig. 14. In this figure, the black dot on each of the frequency curves indicates the lowest observed frequency in the respective mode (See Table 2). The numerical frequencies at the left represent the analytical natural frequencies for case when the median stiffness is zero and is the assymptote for the frequency curves f_1 through f_5. This figure shows that, especially in the higher modes, relatively slight variations in median stiffness can account for a multiplicity of frequencies in a given mode.

In Fig. 12 the observed 2.08 hz fundamental mode (b) lies between curves (a) and (c) with median stiffness of zero and five. This lowest experimental fundamental frequency also lies in this stiffness range in Fig. 14. The 2.32 hz observed fundamental mode is approximated by the analytical curve (d) at the top of Fig. 12 with a median stiffness of 100. Both the f_1 frequency curve in Fig. 14 and curve (d) in Fig. 12 indicate that the median restraint in this mode is greater than 100. In addition, the other mode shapes shown in Figs. 12 and 13 indicate that the analytical mode shape that agrees best with the experimentally determined mode is associated with a median stiffness from Fig. 14 that is in reasonable agreement with that indicated by the mode shape comparison.

Even though the simple elastic action of the median is a very rough approximation of the complex way in which the presence of the median strip affects the transverse motions of Ramp 13, it is clear that the action of the median strip at these relatively small vibration amplitudes is the explanation for the nonunique dynamic behavior observed. Figures 12 and 13 show that the multiple shapes observed within a mode can be explained in this way; but more importantly, Figs. 12 and 13 along with the frequency plot in Fig. 14, indicate that not only are the shapes explained but also their associated frequencies.

C. VERTICAL MOTION

The data points in Fig. 15 experimentally define the first four mode shapes for the vertical sense of motion. The experimental results for the vertical motion study (10) was obtained by using the same station layout and analysis techniques, as indicated in chapter 3 of this report. Traffic induced vertical motions rather than quick release vibrations were used for vertical motion analysis; consequently no reliable damping estimates were obtained. The experimental points in Fig. 15 were calculated from vertical accelerograms obtained while the vehicle causing the motion was still on the bridge.

The solid envelope curves in Fig. 15 represent the envelopes of all computed vertical mode shapes. The models used in this envelope computation include treating the deck as a composite section with the deck regarded as acting fully composite with the three girders over the full length of the bridge. A second model treats the deck plus concrete rails acting fully composite with the girders. In both of these cases, the modulus of elasticity of the concrete was varied over a wide range (Fig. 16). Also included, was the case where the individual girders were regarded as acting separately with the tributary deck concrete acting composite with them. In addition, a model was used in which the concrete in the negative moment regions over the piers where the shear connectors are spaced at two foot intervals, was removed

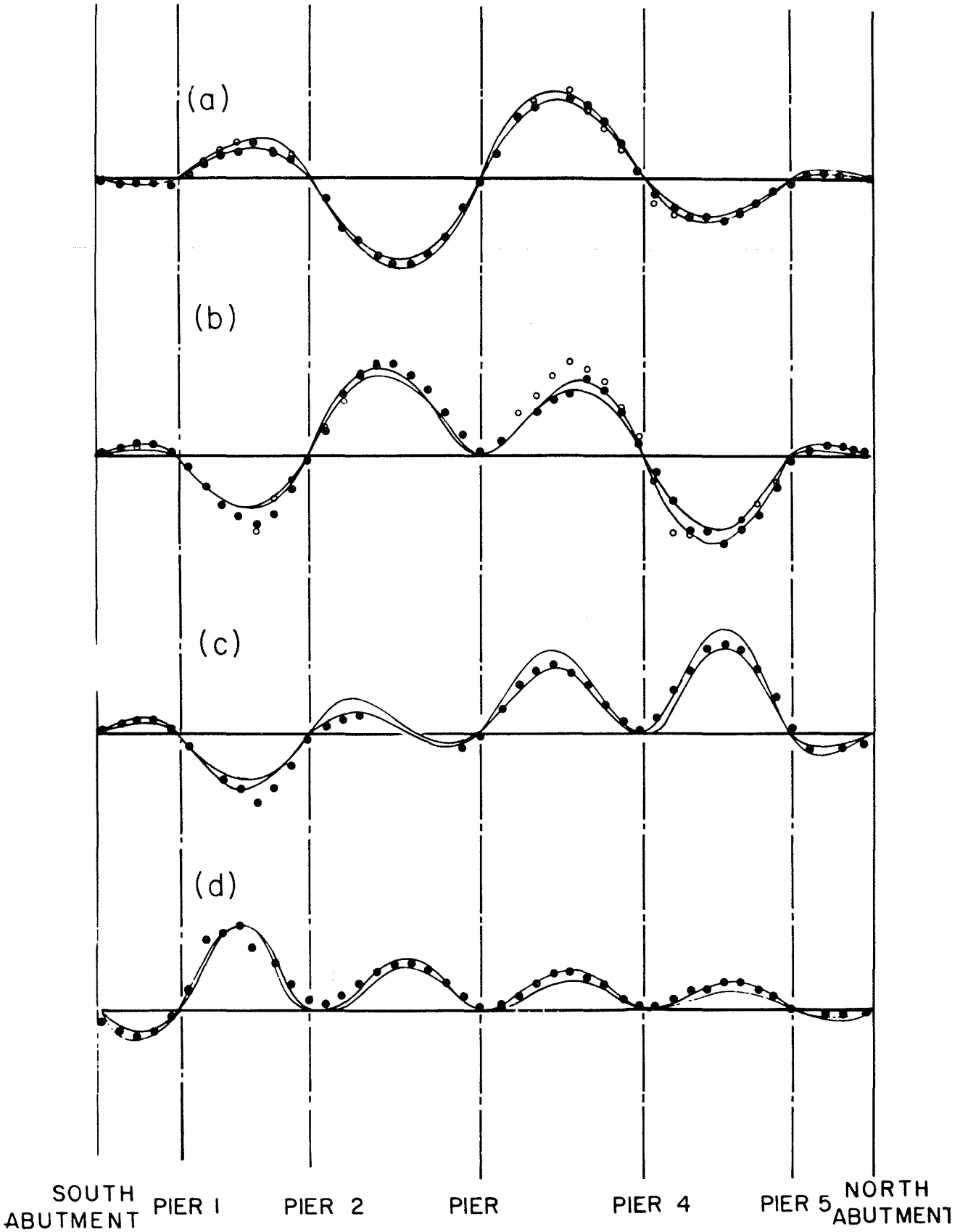

Fig. 15 Vertical Mode Shapes

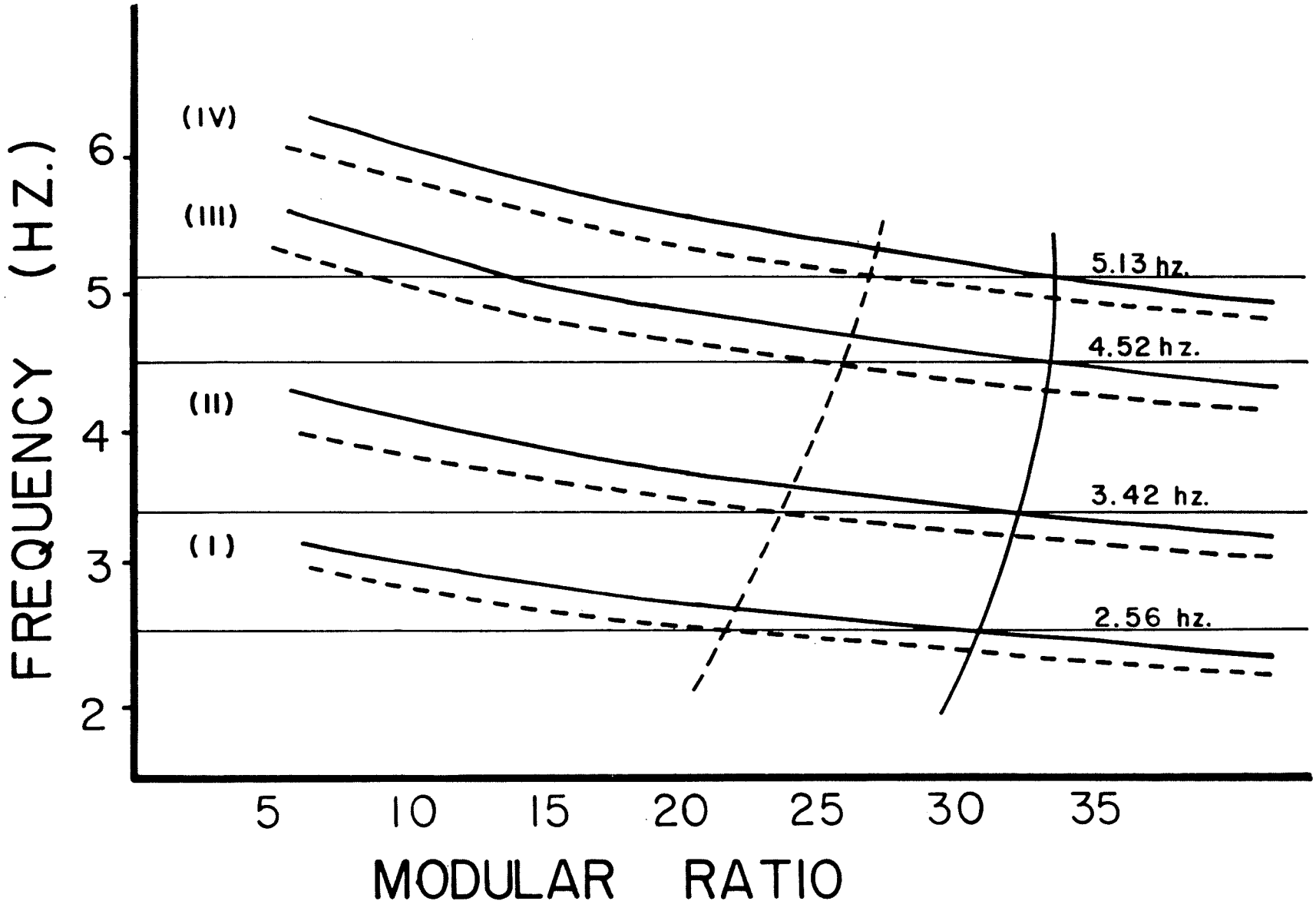

Fig. 16 Vertical Natural Frequencies Versus Modular Ratio

entirely. In this case, the modulus of elasticity of 4000 psi deck concrete at the center of the spans where full composite action is expected, was taken at its full instantaneous load value. The envelope mode shapes in Fig. 15 computed from these models can be seen to be in excellent agreement with the experimental mode shapes. From this and the agreement of theoretical and experimental frequency ratios (Fig. 16), it is clear that the presence of the vehicle on the bridge causing the vertical motion did not affect the results.

Fig. 16 is a plot of the first four vertical theoretical natural frequencies versus the modular ratio, where modular ratio is defined as the ratio of the modulus of elasticity of the girder steel to the modulus of elasticity of the deck concrete. For 4000 psi concrete, the modular ratio for full composite action for instantaneous loading is 8. In Fig. 16 the upper solid curves represent plots of natural frequency versus modular ratio for the case where the deck and rails were regarded as acting as composite with the girders. The lower dashed curves are associated with the case when the deck without rails was used. The horizontal lines at 2.56 hz, 3.42 hz, 4.52 hz, and 5.13 hz are the observed vertical natural frequencies. In this figure, the vertical solid black line represents the intersection of the observed natural frequencies with the theoretical natural frequency curves computed when both the railing and the deck were treated as acting composite with the steel girders. In this case, the

effective modular ratio varies between 30 and 33, and the observed ratios of the first four natural frequencies is in excellent agreement with the theoretical natural frequency ratios. The dashed vertical curve in Fig. 16 represents the intersection of the experimental natural frequencies with theoretical frequencies for the case where the deck alone was regarded as acting compositely with the girders. In this case, the effective modular ratio ranged between 21 and 26.

The excellent agreement between theoretical and experimental mode shapes (Fig. 14) and the results shown in Fig. 15 suggests that continuous composite girders which have provision for full composite action only in the central portion of the spans may be treated analytically as being continuously composite if an increased modular ratio is used. In the structure studied, the ultimate strength of the deck concrete was 4000 psi, and the associated modular ratio for instantaneous deflections is 8. Experimental results in Fig. 16 indicate that the effective modular ratio should be on the order of 27 to analytically describe Ramp 13's vertical stiffness. This is on the order of three times the modular ratio for fully composite action with instantaneous deformation.

V. EARTHQUAKE RESPONSE

A. ANALYTICAL MODEL.

To estimate Ramp 13's seismic response, the analytical model of the structure without median strip was used. Since the experimental transverse displacements were small, the median strip was capable of restraining the bridge during the tests; but for the larger motions expected during earthquakes, it would not be expected to substantially restrain the structure. The natural frequencies of the system used are listed in Table 4, and are also shown in Fig. 14. The

Table 4. Natural Frequencies

Mode	1	2	3	4	5
Frequency	1.8	2.6	4.6	7.2	9.3

experimental damping ratios obtained were in the range of 1.5 to 4 percent of critical. To account for the possibility of higher damping ratios associated with larger motions, all seismic response calculations were made for modal damping ratios of 2 percent and 5 percent of critical.

B. STATIC RESPONSE.

For purposes of comparison with the earthquake response results, the static lateral forces delivered to the piers and the abutments by the 0.3 K/ft. wind load, which controlled in the design, were computed. These lateral wind

forces are listed in column 6 of Table 5. The associated bending moments, reactions, displacements and center line geometry of the pier frames are also listed in this table. The total dead load reaction delivered to each pier by the deck superstructure is shown in column 7. The longitudinal static response of piers 3 and 4, (the only piers resisting longitudinal load) due to the 4 percent g earthquake load required by the 1961 AASHO specifications for this bridge is also shown.

C. INPUT GROUND MOTIONS AND RECURRENCE TIMES.

Since the analytical model used is linear and appropriate only for relatively small ground motions, five accelerograms recorded primarily on soft sites were selected (6) which could be expected to occur at least several times in the lifetime of the structure. The Ramp 13 bridge structure is founded on an intermediate to soft site, where the classification of the geology at a site as hard, intermediate or soft suggested by Trifunac and Brady (25) was followed. Their published site classifications (25) for the five accelerograms used in this study was adopted. These accelerograms are shown in Fig. 17, and their properties including their approximate recurrence times in Western Nevada are indicated at the top of Tables 6 through 10. In each case, the lower recurrence time is appropriate for dynamic analyses in which the peak response occurs early in the time history and the duration

TRANSVERSE STATIC RESPONSE (300#/ft. Wind)

Pier No.	H (in)	W (in)	M_B (Kip·in)	M_T (Kip·in)	F (Kip)	R_{DL} (Kip)	R (Kip)	Δ (in)
S. Abut.					18.6	71.3		.0093
Pier 1	362	168	875.0	891.0	9.76	256.0	10.6	.0976
Pier 2	373	168	1636.0	1665.0	17.7	406.0	19.8	.1915
Pier 3	360	168	3235.0	3119.0	35.3	456.0	37.1	.1960
Pier 4	341	168	2596.0	2502.0	29.9	413.0	29.8	.1439
Pier 5	297	168	748.0	767.0	10.2	308.0	9.13	.0599
N.Abut.					13.0	29.5		.0065

1940 ≡ Total DL Superstructure

LONGITUDINAL STATIC RESPONSE (4% EQ)

Pier No.	M_B (Kip·in)	F (Kip)	Δ (inches)
Pier 3	6624.0	36.8	.652
Pier 4	7351.0	43.24	.652

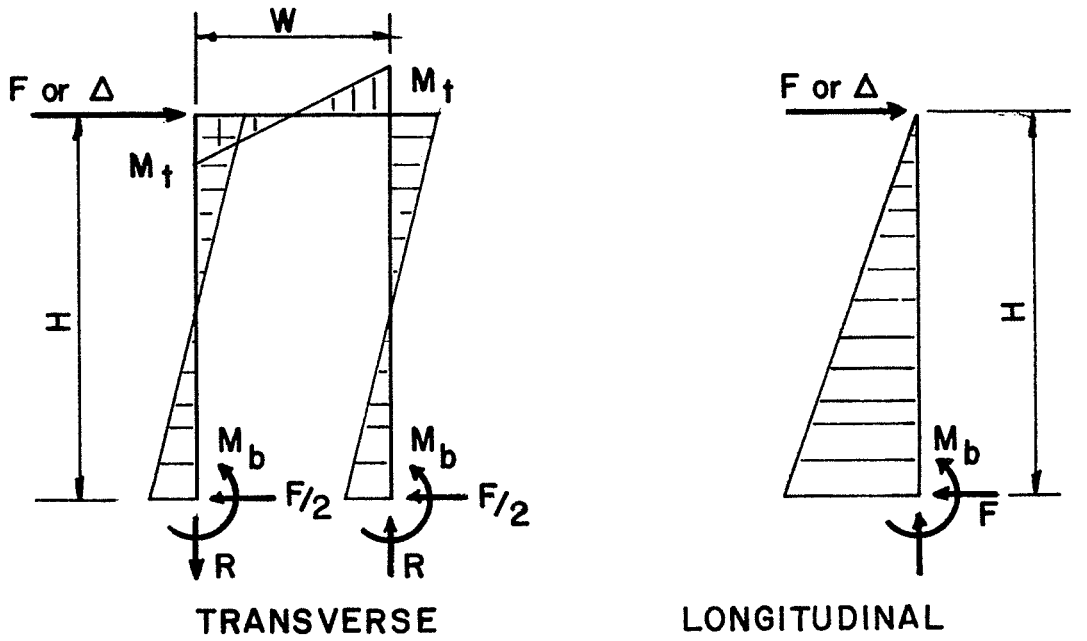

TABLE 5 Static Response Results

of shaking from the onset of the record is short. The longer recurrence times are appropriate for the full duration accelerograms.

Fig. 18 from Douglas and Ryall (9) shows the curve from which recurrence times were estimated, and is appropriate for the average seismicity of Western Nevada. One of the principal assumptions that entered into the development of these curves was that it is equally likely that earthquakes can occur anywhere in the region, which is reasonable for the more or less homogeneous distribution of faulting and earthquake activity in Western Nevada. Seven hundred earthquakes having a Richter magnitude greater than 4 occurring in a 38 year period in a 33,000 square mile zone were used for developing the earthquake recurrence rates used in developing this result. In Fig. 18, â is a peak rock acceleration expected at the site, T is recurrence time in years for the peak acceleration to equal or exceed â. M is Richter magnitude, and D is Housner's (28) duration of shaking in seconds. The recurrence time for peak acceleration to exceed â caused by all earthquakes having a magnitude of 5 or greater is read off the left hand scale for M = 5. If it is desired to find the recurrence time for peak acceleration to exceed $\hat{a}$ caused by all earthquakes having a magnitude greater than M = 6 then the recurrence times are read from the scale where â intersects M = 6. For example, peak accelerations exceeding 0.15 g caused by all earthquakes greater than M = 5 occur about

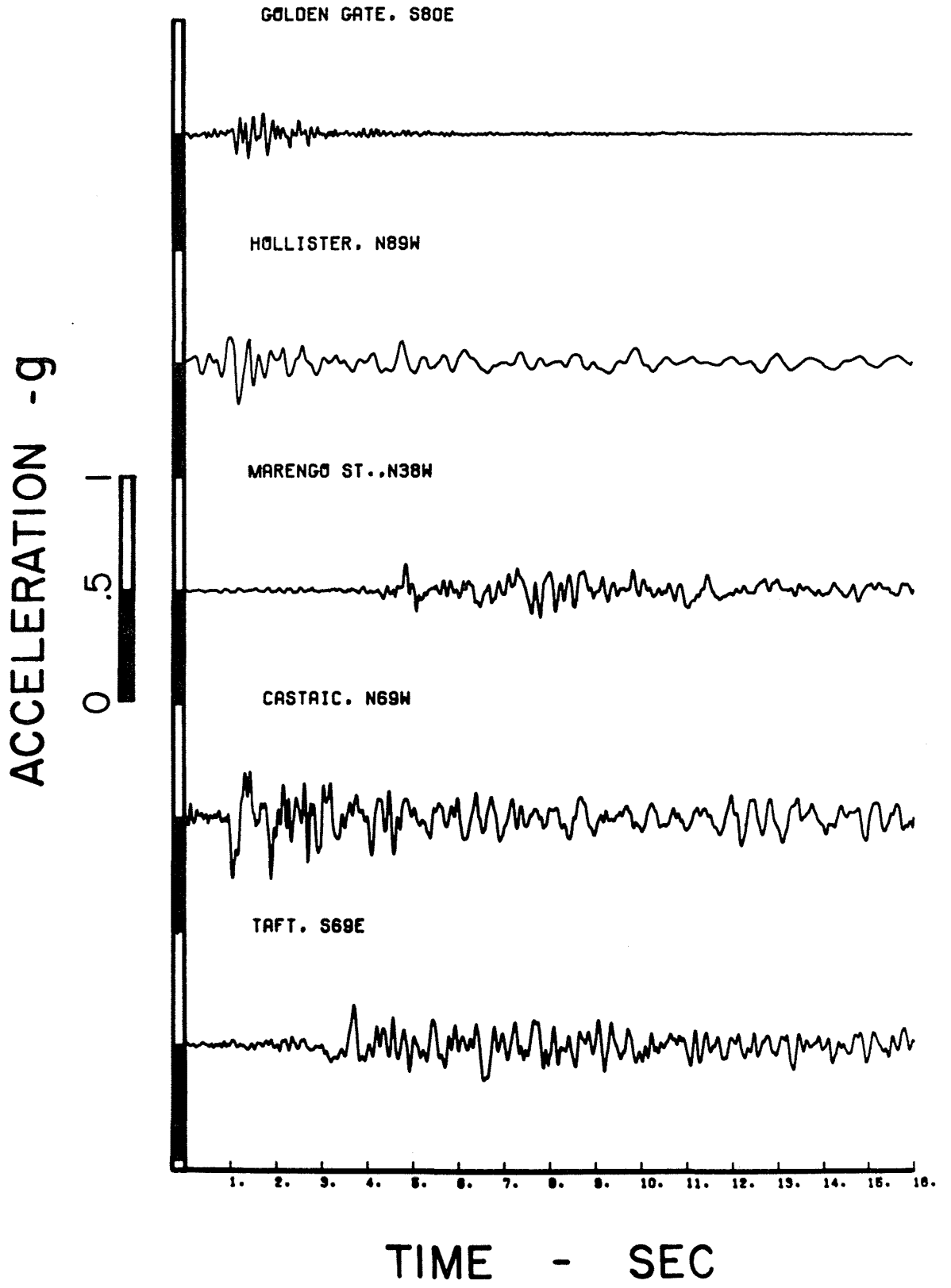

Fig. 17 Accelerograms Used for Earthquake Response Calculations

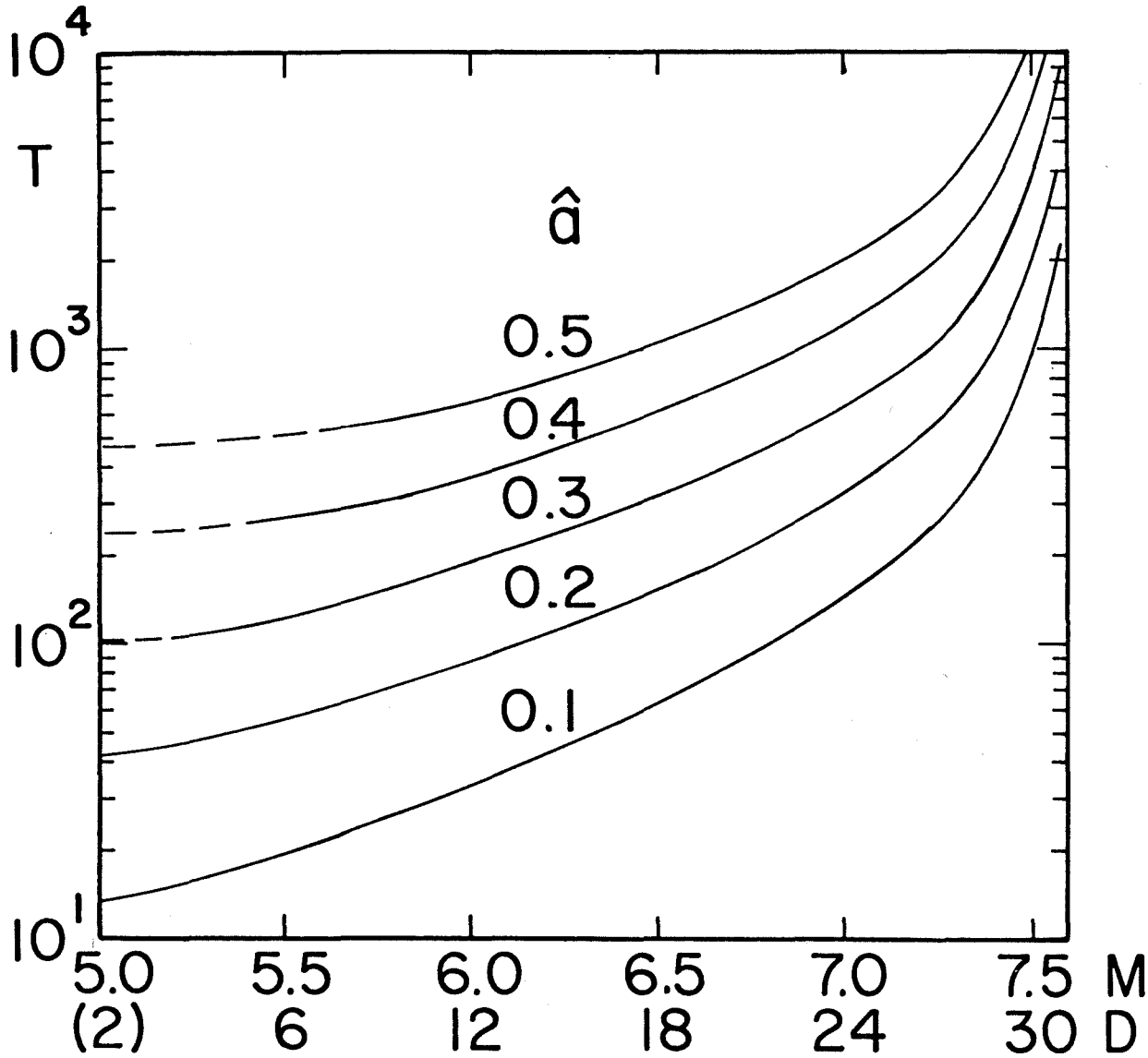

Fig. 18 Return Period For Peak Acceleration Versus Causal Earthquake Magnitude From Reference 9

every 20 or 30 years, while longer duration strong ground shaking having peak accelerations greater than 1/2 g caused by all earthquakes having Richter magnitudes greater than 6 1/2 would be on the order of one thousand years.

Two recurrence times for each of the accelerograms shown in Fig. 17 were estimated. The shorter recurrence times indicated in Tables 6 to 10 were obtained by using the recorded peak acceleration and a magnitude of 5. In this case, it was assumed that the first few seconds of the accelerogram would be representative of ground motions caused by the smaller earthquakes having a Richter magnitude of 5 or greater. The longer recurrence times shown were estimated by using the recorded peak acceleration and the actual earthquake magnitude for the accelerogram. In both cases, the soil interaction problem was ignored. It was assumed that recurrence estimates based on peak rock acceleration and peak ground accelerations including the soil response were the same. Attempting to include the soil response in making these recurrence time estimates would be well beyond the scope of the present study.

D. RESPONSE RESULTS

Tables 6 through 10 summarize the peak dynamic responses caused by each of the five accelerograms for damping ratios of two and five percent of critical. In the tables of transverse results, the peak transverse dynamic displacement of the piers is listed in column 5. Column 6 gives the time at

which the peak response occurs, and column 4 gives the ratio of the dynamic pier forces and displacements to the design wind load levels as indicated in Table 5. The M_b ratio in column 3, is the ratio of the elastic dynamic moment at the base of the pier column to the ultimate moment capacity of the column. Column 2 lists the ratio of the dynamic pier force transmitted to each steel diaphram frame compared to the allowable force on each frame as dictated by the non-moment resisting friction type bolted joints of the frame.

In the tables (see Tables 6-11) of longitudinal response parameters, Δ is the longitudinal displacement in inches, F is the ratio of the peak longitudinal pier force to the static force caused by the 4 percent g design earthquake force (Table 5), and M_b is the ratio of the peak longitudinal dynamic moment at the base of the pier column to its ultimate moment capacity. Table 11 gives the average response to all five accelerograms and represents the arithmetic mean of Tables 6 through 10.

Tables 12 and 13 give the peak dynamic transverse responses when the transverse restraints at the abutments have been removed so that all the lateral forces must be resisted by the piers only. This model was introduced in order to estimate the response of the structure if the transverse restraints provided by the rocker failed.

The average responses caused by all five earthquake accelerograms are tabulated in Table 11. The recurrence time for this "average" earthquake would be from 30 to 100 years

in Western Nevada depending upon whether the first few seconds of shaking are used, or whether the full duration of shaking is used. Since the maximum structural responses occurred within the first few seconds after the beginning of strong motion, the 30 year recurrence time is appropriate. In this situation, the early portion of the accelerograms is used to approximate the effect of smaller earthquakes. These are the ground motions that could be expected to occur a few times within the lifetime of the structure, and for which the structural response could be expected to be in the linear range.

The peak ground motion parameters associated with this "average" earthquake associated with the results in Table 11 are as follows:

peak acceleration = 0.17 g,

peak velocity = 6.15 in/sec, and

peak displacement = 2.8 inches.

These peak ground motions are about 14 percent of the largest ground motions ever recorded at Pacoima Dam during the 1971 San Fernando earthquake.

In Table 11, column 2, it is apparent that the dynamic forces on the diaphram frames are substantially in excess of the allowable levels, particularly at the central piers and at the abutments. Even in the case of the 1957 Golden Gate San Francisco accelerogram (Table 6), which was the smallest ground motion used, the diaphram forces at the abutments are 2.5 to 4 times their allowable levels. For this small input accelerogram it can be seen from Table 6 that the pier forces

are in general less than the lateral static wind load forces except at the abutments. This illustrates the importance of using dynamic analysis in estimating the distribution of lateral forces even in a relatively simple structural system. In addition, examination of the keeper detail used to prevent transverse displacements of the bottom flange of the girder with respect to the top of the 1 foot deep rocker is inadequate. These keepers are small 3 by 2.5 by 0.5 inch plates welded to the bottom flange of the girder and provide for only a nominal restraint. These keepers would be loaded well beyond their capacity, particularly in the short end spans where vertical response calculations (10) indicate that uplift could be about 50 to 60 percent achieved with the Taft vertical accelerogram of the 1952 Kern County earthquake and the 1971 San Fernando vertical accelerogram recorded at Castaic. The allowable displacement of the bottom girder flange and the keepers is only 1/8 inch. Tables 12 and 13 show that the displacement demand that would be made on them would be in the range of 0.7 to 1.7 inches, which would clearly shear them off and allow the rocker at the abutment girder supports to fall out should uplift of the ends of the bridge deck occur.

From Table 11 it is apparent that the linear theory indicates that the pier frame bending moments at the interior piers will be at or above ultimate moment levels in the transverse sense. In the longitudinal sense, the moments are on the order of twice the ultimate level. These transverse and

longitudinal motions occur simultaneously. The larger longitudinal moments occur because all the longitudinal loads on the structure are carried by piers 3 and 4 only.

It should also be noted that because of the near balance of the transverse moments at the top and bottom of the pier columns (Table 5), the ultimate moments at the top and bottom will be reached at about the same time. This means that pier frames in this condition are in a plastic collapse mode, and provide no further resistance to lateral forces.

GROUND MOTION DATA

Description: 1957 San Francisco Earthquake (Golden Gate S80E)

Magnitude = 5.3 A_{max} = .105 g

Distance to Fault = 7 mi. V_{max} = 1.81 in/sec.

Soil Type = (1) Hard D_{max} = .31 in.

Return Period 14 to 16 years.

In Western Nevada

TRANSVERSE RESPONSE PARAMETERS

Pier	F_d Ratio		M_b Ratio		Δ & F Ratio		Δ (inches)		Time
	2%	5%	2%	5%	2%	5%	2%	5%	
S. Abut.	4.07	2.89			3.35	2.33	.0312	.0216	1.1
Pier 1	.52	.341	.165	.109	1.80	1.18	.176	.115	1.3
Pier 2	.778	.608	.255	.200	1.48	1.16	.284	.222	1.5
Pier 3	1.54	1.20	.380	.298	1.47	1.15	.289	.225	1.1
Pier 4	.906	.79	.212	.186	1.02	.896	.147	.129	.9
Pier 5	.578	.42	.151	.110	1.92	1.40	.115	.0837	.8
N.Abut.	3.36	2.42			3.95	2.85	.0257	.0185	.8

LONGITUDINAL RESPONSE PARAMETERS

Pier	F Ratio		M_b Ratio		Δ (in)	
	2%	5%	2%	5%	2%	5%
Pier 3	.67	.58	.358	.308	.44	.38
Pier 4	.67	.58	.397	.342	.44	.38

Table 6 Dynamic Response Results for 1957 San Francisco Earthquake Recorded at Golden Gate

GROUND MOTION DATA

Description: 1961 Hollister Earthquake (City Hall N 89 W)

Magnitude = 5.6
Distance to Fault = 9 mi
Soil Type = (0) Soft
Return Period 35 to 50 years
In Western Nevada

A_{max} = .18 g
V_{max} = 6.73 in/sec.
D_{max} = 1.49 in.

TRANSVERSE RESPONSE PARAMETERS

Pier	F_d Ratio		M_b Ratio		Δ & F Ratio		Δ (inches)		Time
	2%	5%	2%	5%	2%	5%	2%	5%	
S.Abut.	6.34	5.14			5.22	4.23	.0485	.0393	1.7
Pier 1	2.04	1.52	.649	.485	7.05	5.27	.688	.514	3.1
Pier 2	3.93	2.93	1.29	.96	7.51	5.59	1.438	1.071	3.1
Pier 3	7.30	5.53	1.81	1.37	6.98	5.30	1.370	1.038	3.1
Pier 4	5.67	3.77	1.33	.885	6.40	4.26	.922	.613	3.4
Pier 5	1.62	1.08	.422	.283	5.36	3.59	.321	.215	3.4
N.Abut.	3.72	2.86			4.37	3.37	.0284	.0219	1.3

LONGITUDINAL RESPONSE PARAMETERS

Pier	F Ratio		M_b Ratio		Δ (in.)	
	2%	5%	2%	5%	2%	5%
Pier 3	5.52	4.29	2.93	2.28	3.6	2.8
Pier 4	5.52	4.29	3.25	2.52	3.6	2.8

Table 7 Dynamic Response Results for 1961 Hollister Earthquake Recorded at City Hall

GROUND MOTION DATA

Description: 1971 San Fernando Earthquake (First Floor 1640 Marengo St., N38W)

Magnitude = 6.6 A_{max} = .12g

Distance to Fault = 20 mi. V_{max} = 6.34 in/sec.

Soil Type = (0) Soft D_{max} = 4.72 in.

Return Period 16 to 87 years

In Western Nevada

TRANSVERSE RESPONSE PARAMETERS

Pier	F_d Ratio		M_b Ratio		Δ & F Ratio		Δ (inches)		Time
	2%	5%	2%	5%	2%	5%	2%	5%	
S.Abut.	5.50	4.23			4.52	3.48	.0421	.0324	4.7
Pier 1	1.39	1.11	.443	.353	4.81	3.83	.469	.374	4.4
Pier 2	2.58	2.10	.849	.692	4.93	4.02	.945	.770	4.4
Pier 3	5.46	4.25	1.36	1.06	5.25	4.08	1.03	.799	4.1
Pier 4	4.00	3.22	.939	.75	4.52	3.62	.650	.522	3.7
Pier 5	1.27	1.01	.332	.265	4.22	3.37	.253	.202	3.7
N.Abut.	2.90	2.46			3.42	2.89	.0222	.0188	4.8

LONGITUDINAL RESPONSE PARAMETERS

Pier	F Ratio		M_b Ratio		Δ (in.)	
	2%	5%	2%	5%	2%	5%
Pier 3	5.52	3.98	2.93	2.11	3.6	2.6
Pier 4	5.52	3.98	3.24	2.34	3.6	2.6

Table 8 Dynamic Response Results for 1971 San Fernando Earthquake Recorded at 1640 Marengo Street

GROUND MOTION DATA

Description: 1971 San Fernando Earthquake (Castaic N69W)

Magnitude = 6.6 A_{max} = .27 g

Distance to Fault = 18 mi. V_{max} = 10.7 in/sec.

Soil Type = (1) Hard D_{max} = 3.66 in.

Return Period 80 to 280 years.

In Western Nevada

TRANSVERSE RESPONSE PARAMETERS

Pier	F_d Ratio		M_b Ratio		Δ & F Ratio		Δ (inches)		Time
	2%	5%	2%	5%	2%	5%	2%	5%	
S. Abut.	11.4	7.20			9.35	5.92	.087	.0551	3.5
Pier 1	4.45	2.76	1.42	.88	15.4	9.56	1.50	.933	4.0
Pier 2	8.5	5.26	2.79	1.72	16.2	10.0	3.10	1.92	4.0
Pier 3	16.1	10.3	3.99	2.55	15.4	9.84	3.01	1.93	4.0
Pier 4	11.9	7.59	2.78	1.78	13.4	8.55	1.93	1.23	.5
Pier 5	3.46	2.15	.898	.56	11.4	7.13	.68	.427	.5
N.Abut.	5.22	4.43			6.15	5.22	.0400	.0339	2.1

LONGITUDINAL RESPONSE PARAMETERS

Pier	F Ratio		M_b Ratio		Δ (in)	
	2%	5%	2%	5%	2%	5%
Pier 3	5.52	4.91	2.93	2.60	3.6	3.2
Pier 4	5.52	4.91	3.24	2.88	3.6	3.2

Table 9 Dynamic Response Results for 1971 San Fernando Earthquake Recorded at Castaic

GROUND MOTION DATA

Description: 1952 Kern County Earthquake (Taft S69E)

Magnitude = 7.7 A_{max} = .18 g

Distance to Fault = 30 mi. V_{max} = 6.96 in/sec.

Soil Type = (0) Soft D_{max} = 3.62 in.

Return Period 34 to 400 years.

In Western Nevada

TRANSVERSE RESPONSE PARAMETERS

Pier	F_d Ratio		M_b Ratio		Δ & F Ratio		Δ (inches)		Time
	2%	5%	2%	5%	2%	5%	2%	5%	
S.Abut.	8.10	5.21			6.66	4.30	.0620	.040	5.2
Pier 1	2.37	1.64	.755	.524	8.20	5.69	.800	.555	5.2
Pier 2	4.26	2.99	1.39	.980	8.09	5.69	1.56	1.09	5.1
Pier 3	8.58	5.78	2.12	1.43	8.21	5.51	1.61	1.08	5.1
Pier 4	5.73	4.10	1.34	.959	6.46	4.62	.930	.665	4.8
Pier 5	1.86	1.17	.481	.306	6.11	3.89	.366	.233	5.6
N.Abut.	5.03	3.47			5.92	4.08	.0385	.0265	6.7

LONGITUDINAL RESPONSE PARAMETERS

Pier	F Ratio		M_b Ratio		Δ (in)	
	2%	5%	2%	5%	2%	5%
Pier 3	3.98	3.22	2.11	1.71	2.6	2.1
Pier 4	3.98	3.22	2.34	1.89	2.6	2.1

Table 10 Dynamic Response Results for 1952 Kern County Earthquake Recorded at Taft.

GROUND MOTION DATA

Description:

Magnitude = 6.4 A_{max} = .17 g

Distance to Fault = 17 mi. V_{max} = 6.5 in/sec.

Soil Type = (0) Soft D_{max} = 2.8 in

Return Period 32 to 100 years

In Western Nevada

TRANSVERSE RESPONSE PARAMETERS

Pier	F_d Ratio		M_b Ratio		Δ & F Ratio		Δ (inches)		Time
	2%	5%	2%	5%	2%	5%	2%	5%	
S.Abut.	7.1	4.9			5.8	4.1	0.54	.038	3.2
Pier 1	2.2	1.5	.69	.47	7.5	5.1	.72	.50	3.6
Pier 2	4.0	2.8	1.3	.91	7.6	5.3	1.5	1.0	3.6
Pier 3	7.8	5.4	1.9	1.3	7.5	5.2	1.5	1.0	3.5
Pier 4	5.6	3.9	1.3	.91	6.4	4.4	.91	.63	2.7
Pier 5	1.8	1.2	.46	.30	5.8	3.9	.35	.23	2.8
N.Abut.	4.0	3.1			4.8	3.7	.031	.024	3.1

LONGITUDINAL RESPONSE PARAMETERS

Pier	F Ratio		M_b Ratio		Δ (in)	
	2%	5%	2%	5%	2%	5%
Pier 3	4.2	3.4	2.3	1.8	2.8	2.2
Pier 4	4.2	3.4	2.5	2.0	2.8	2.2

Table 11 Average Response Results (Average of Tables 6-10)

GROUND MOTION DATA

Description: 1961 Hollister (City Hall, N89W)

Magnitude = 5.6 A_{max} = .18 g

Distance to Fault = 9 mi. V_{max} = 6.73 in/sec.

Soil Type = (0) Soft D_{max} = 1.49 in.

Return Period 35 to 50 years.

In Western Nevada

TRANSVERSE RESPONSE PARAMETERS

Pier	F_d Ratio		M_b Ratio		Δ & F Ratio		Δ (inches)		Time
	2%	5%	2%	5%	2%	5%	2%	5%	
S.Abut.	---	0	---	---	---	0	---	1.70	5.4
Pier 1	---	3.84	---	1.23	---	13.3	---	1.30	5.4
Pier 2	---	2.85	---	.935	---	5.43	---	1.040	5.0
Pier 3	---	4.16	---	1.03	---	3.98	---	.781	5.2
Pier 4	---	4.92	---	1.15	---	5.56	---	.799	3.0
Pier 5	---	4.44	---	1.16	---	14.7	---	.885	3.0
N.Abut.	---	0	---	----	---	0	---	1.00	3.0

LONGITUDINAL RESPONSE PARAMETERS

SAME AS TABLE 7.

Table 12 Dynamic Response Results When the Transverse Supports at the Abutments are Removed - 1961 Hollister Earthquake at City Hall.

GROUND MOTION DATA

Description: 1971 San Fernando (First Floor 1640 Marengo St., N38W)

Magnitude = 6.6 A_{max} = .12 g

Distance To Fault = 20 mi. V_{max} = 6.34 in/sec.

Soil Type = (0) Soft D_{max} = 4.72 in.

Return Period 16 to 87 years.

In Western Nevada

TRANSVERSE RESPONSE PARAMETERS

Pier	F_d Ratio		M_b Ratio		Δ & F Ratio		Δ (inches)		Time
	2%	5%	2%	5%	2%	5%	2%	5%	
S. Abut.	---	0	---	---	---	0	---	1.37	8.0
Pier 1	---	3.19	---	1.01	---	11.0	---	1.08	8.0
Pier 2	---	2.09	---	.687	---	3.99	---	.765	8.0
Pier 3	---	2.54	---	.629	---	2.43	---	.477	8.0
Pier 4	---	2.91	---	.683	---	3.29	---	.473	4.4
Pier 5	---	2.90	---	.757	---	9.61	---	.577	4.6
N.Abut.	---	0	---	----	---	0	---	.676	4.6

LONGITUDINAL RESPONSE PARAMETERS

SAME AS TABLE 8.

Table 13 Dynamic Response Results When the Transverse Supports at the Abutments are Removed - 1971 San Fernando Earthquake at 1640 Marengo Street

VI. CONCLUSIONS

1. Quick release pullback testing is an effective method of identifying the structural dynamic characteristics (natural frequencies mode shapes, and modal damping ratios) of bridge structures. The method is particularly attractive for experimental testing of bridge structures because data can be obtained during lulls in traffic. Even in the case where the traffic on the structure is heavy, the quick release pullback testing approach would mean that traffic would only have to be stopped for very brief periodic intervals to obtain the necessary data. Resonance testing would involve the closure of the structure to traffic for more sustained periods of time. In addition, the cost of acquiring field data would be low compared to resonance testing.

2. More physical testing of various classes of bridge structures should be undertaken to identify their dynamic characteristics in the field. Vibration amplitudes should be varied in order to determine the effect of vibration amplitude on these properties. Achieving the desired experimental amplitudes with the quick release method is relatively simple, and by carefully studying the effects of low amplitude vibrations, safe larger vibration amplitudes could be selected. The ideal time to select a bridge for this form of physical testing would be in the design phase. The quick release dynamic loads are well defined so it would be a relatively simple matter for the designer to estimate their effect upon

the structure at any desired amplitude level. In addition, simple pick up points for attaching the loading cable could be provided.

3. The soil structure interaction problem should be considered at least in an approximate manner if a detailed soil structure interaction dynamic analysis is not performed. In the case of Ramp 13, the analytical results were sensitive to the modulus of subgrade reaction used to approximate the soil structure interaction effects.

4. In composite girder construction, the details used to transmit the lateral loads from the deck superstructure to piers and abutments need a complete review. In particular, the diaphram frames should be moment resisting of adequate capacity. Also the rocker bearing details need adequate restrainers to prevent excessive displacements and their use eliminated wherever possible.

5. Relatively too much emphasis has been placed on vertical and thermal loads compared to the seismic forces. Care should be exercised to insure that the capacity of bridge structures to resist seismic forces should be more balanced in the transverse and longitudinal directions.

6. The earthquake forces specified in the 1961 AASHO code under which this structure was designed are too low for Western Nevada and other areas of comparable seismicity. Bridges similar to the one studied herein, can be expected to sustain some seismic structural damage every 30 to 40 years in areas with seismicity comparable to Western Nevada,

and would probably collapse in the event of a maximum credible earthquake.

7. In seismic areas comparable to Western Nevada, a review of all important bridges designed under the AASHO earthquake regulation* should be undertaken for purposes of making possible retrofit recommendations regarding their seismic performance.

8. Vehicular traffic induced motions can be used to effectively identify the vertical mode shapes and natural frequencies. Analysis of vertical motion, data obtained from Ramp 13 strongly suggests that the vertical stiffness of composite girder bridges can be estimated by treating them as continuously composite with an increased effective modular ratio applied uniformly over the whole bridge deck. No special account need be taken of the fact that little composite action occurs over the piers in the negative moment regions other than using this increased effective modular ratio.

---

*EQ = CD
where
EQ = Lateral force applied horizontally in any direction at center of gravity of the weight of the structure.
D = Dean load of structure.
C = 0.02 for structures founded on spread footings on material rated as 4 tons or more per square foot.
= 0.04 for structures founded on spread footings on material rated as less than 4 tons per square foot.
= 0.06 for structures founded on piles.

BIBLIOGRAPHY

1. Barkan, D.D., Dynamics of Bases and Foundations, McGraw-Hill Book Co., New York, N.Y., 1962, 424 pp.

2. Bathe, K.J., Wilson, E.L., and Peterson, F.E., "SAP IV A Structural Analysis Program for Static and Dynamic Response of Linear Systems," Univ. of Calif. Berkeley, EERC Report 73-11, 1973, Revised 1974, 60 pp.

3. Benuska, K.L., "Structural Vibration Survey of a Multi-story Pyramid-Shaped Building Using Ambient Wind Vibrations," Report to the Department of Civil Engineering University of California, Berkeley, 1973. (Reproduced as an appendix in Ref. 10)

4. Bracewell, R. The Fourier Transform and Its Applications, McGraw-Hill Book Co., New York, N.Y. 1965.

5. California Institute of Technology, "Analysis of Strong Motion Earthquake Accelerograms," Vol. IV, Part A., EERL Report 72-100, 1972, pp 1-38.

6. California Institute of Technology, Strong Motion Earthquake Accelerograms, Vol. II, Part A, EERL 71-50, 1971: Vol. II, Part C., EERL 72-51, 1973; Vol. II, Part D, EERL 72-52, 1973.

7. Chen, M. and Penzien, J., "Analytical Investigations of Seismic Response of Short, Single, or Multiple Span Highway Bridges;" Univ. of Calif. Berkeley, EERC Report 75-4, 1975, 163 pp.

8. Cooley, J.W. and Tukey, J.W., "An Algorithm for the Machine Calculation of Comples Fourier Series," Mathematical Computation, Vol. 19, 1965, pp 297-301.

9. Douglas, B.M. and Ryall, A.S., "Return Periods for Rock Acceleration in Western Nevada," Bull. Seism. Soc. of Amer., Dec. 1975, (In Press)

10. Fricke, H.F., "Traffic Induced Dynamics of a Highway Bridge," M.S. Thesis, Department of Civil Engineering, Univ. of Nevada, Reno, Nevada (In preparation).

11. Fung, G.G., LeBeau, R.J., Klein, E.D., Belvedere, J., and Goldschmidt, A.F., "The San Fernando Earthquake - Field Investigation of Bridge Damage," State of California, Business and Transportation Agency, Department of Public Works, Division of Highways, Bridge Department, 1971, 209 pp.

12. Godden, W.G., "Experimental Investigations of the Seismic Behavior of Highway Bridges," FCP Research and Development Conference, U.S. Department of Transportation, Federal Highway Administration, Minneapolis, Minnesota, 1975, Program.

13. Hart, G.C., DiJulio, R.M., and Lew, M., "Torsional Response of High-Rise Buildings," Journal of the Structural Division, ASCE, Vol. 101, No. ST2., Feb. 1975, pp. 397-416.

14. Hart, G.C., and Vasudevan, R., "Earthquake Desing of Buildings: Damping," Journal of the Structural Division, ASCE, Vol. 101., ST 1, Jan. 1975, pp 11-30.

15. Hidalgo, P., and Clough R.W., "Earthquake Simulator Study of a Reinforced Concrete Frame," Univ. of Calif. Berkeley, EERC Report 74-13, 1974, 266 pp.

16. Iwasaki, T., Penzien, J., and Clough, R., "Literature Survey - Seismic Effects on Highway Bridges," Univ. of Calif. Berkeley, EERC Report 72-11, 1972, 310 pp.

17. Jennings, P.D., Ed., "Engineering Features of the San Fernando Earthquake February 9, 1971," Calif. Inst. of Tech., EERL Report 71-02, 1971, pp. 336-443.

18. Richart, F.E., Hall, J.R., and Woods, R.D., Vibrations of Soils and Foundations, Prentice-Hall, Inc., Englewood Cliffs, N.J., 1970, pp 308-380.

19. Shepherd, R. and Charleson, A.W., "Experimental Determination of the Dynamic Properties of a Bridge Substructure," Bull. Seism. Soc. of Amer., Vol. 61, No. 6, December, 1971 pp. 1529-1548.

20. Shepherd, R. and Sidwell, G.K., "Investigations of the Dynamic Properites of Five Concrete Bridges," Fourth Australasian Conference on the Mechanics of Structures and Materials, University of Queens-Land; Brisbane, Australia, 1973, pp 261-268.

21. Stephen, R.M., Hollings, J.P., and Bowkamp, J.G., "Dynamic Behavior of a Multistory Pyramid-Shaped Building," Univ. of Calif. Berkeley, EERC Report 73-17, 1974, 99 pp.

22. Taoka, G.T., Hogan, M., Khan, F. and Scanlan, R.H. "Ambient Response of Some Tall Structures," Journal of the Structural Division, ASCE, Vol. 101 No. ST 1. Jan. 1975, pp 49-65.

23. Thomson, W.T., Vibration Theory and Applications, Prentice-Hall, Inc. Englewood Cliffs, N.J., 1965, pp 36-50;

24. Trifunac, M.D., "Wind and Microtremor Induced Vibrations of a Twenty-Two Story Steel Frame Building," Calif. Inst. of Tech., EERL Report, 1970, 48 pp.

25. Trifunac, M.D. and Brady, A.G., "On the Correlation of Seismic Intensity Scales with the Peaks of Recorded Strong Ground Motion," Bull. Seism. Soc. of Amer., Vol. 65, No. 1, Feb. 1975, pp 139-162.

26. Trifunac, M.D. and Brune, J.N., "Complexity of Energy Release During the Imperial Valley, California Earthquake of 1940," Bull. Seism. Soc. of Amer., Vol. 60, No. 1, Feb. 1970, pp. 137-160.

27. Tseng, W.S., and Penzien, J., "Analytical Investigations of the Seismic Response of Long Multiple Span Highway Bridges," Univ. of Calif. Berkeley, EERC Report 73-12, 1973, 200 pp.

28. Weigel, R.L., Earthquake Engineering, Prentice-Hall Inc., Englewood Cliffs, N.J., 1970, Chapter 4, pp 75-91.

GPO 912-156